CUMULATIVE YIELDS FROM THE 14-MEV NEUTRON FISSION OF ^{238}U

CUMULATIVE YIELDS FROM THE 14-MEV NEUTRON FISSION OF ^{238}U

By

DAVID JOHN GORMAN, B.Sc.

A Thesis

Submitted to the Faculty of Graduate Studies

in Partial Fulfilment of the Requirements

for the Degree

Doctor of Philosophy

McMaster University

October 1967

DOCTOR OF PHILOSOPHY (1967)
(Chemistry)

McMASTER UNIVERSITY
Hamilton, Ontario

TITLE: Cumulative Yields from the 14-MeV Neutron Fission of ^{238}U

AUTHOR: David John Gorman, B.Sc. (McMaster University)

SUPERVISOR: Professor R. H. Tomlinson

NUMBER OF PAGES: (viii); 98

SCOPE AND CONTENTS:

Isotopic abundances of the elements xenon, krypton, and cesium formed in the 14-Mev neutron fission of ^{238}U have been measured using the mass-spectrometric method. The relative yields of some isotopes of krypton, strontium, zirconium, molybdenum, ruthenium, iodine, xenon, barium, cerium and neodymium were measured using a Ge(Li) detector. The ratios were normalized through isobaric nuclides, and absolute yields were obtained by normalizing the sum of the heavy-mass yields to 100%.

A semi-empirical method has been developed for constructing neutron yield curves. Such a curve was used to obtain a primary-yield curve from the cumulative yields reported here. The results indicate that considerable structure might exist in the primary-yield curve at the higher excitation energy.

ACKNOWLEDGEMENTS

The author wishes to express his sincere gratitude to Professor R. H. Tomlinson for his continued encouragement and guidance throughout the course of this work. As the attitude of the student is determined to a large extent by the attitude of his research director, the author considers himself very fortunate to have had Professor Tomlinson as his director.

Thanks are also due to the members of the supervisory committee, Dr. G. L. Keech, and Dr. R. D. Macfarlane for their helpful suggestions; to Dr. W. B. Clarke for his help in analyzing the rare gas samples; and to Dr. C. W. Tang for his invaluable criticism of the manuscript.

The financial assistance of the National Research Council of Canada, and the British American Oil Company Limited, is gratefully acknowledged.

TABLE OF CONTENTS

LIST OF TABLES

LIST OF ILLUSTRATIONS

CHAPTER 1

GENERAL INTRODUCTION

Nuclear fission is the break-up of a heavy nucleus into two or more lighter nuclei with the release of a large amount of energy. Many of the heaviest elements undergo fission spontaneously, but the process is greatly enhanced by the addition of some excitation energy. Fission has been induced in many heavy elements by bombarding them with neutrons, protons, deuterons, alpha particles, mesons, and gamma rays; however, the most studied fission reactions are the thermal neutron fission of ^{233}U, ^{235}U and ^{239}Pu, and the fast neutron fission of ^{232}Th and ^{238}U.

The sequence of events in fission is believed to be as follows:

1. The incident particle is absorbed by the target nucleus.
2. The compound nucleus splits into two fragments.
3. The fragments emit prompt neutrons and gamma rays.
4. The de-excited fragments decay to stability by emitting beta particles, gamma rays, and in some cases, delayed neutrons.

In this sequence, we distinguish between the fission fragments, which are formed at the instant of scission, and the primary fission products which are formed after the fragments emit prompt neutrons. A fission product may be formed either in independent yield as a primary fission product, or from the beta decay of isobars.

The number of primary products that can be formed is immense. In binary fission, products have been identified with mass numbers as

low as 72 and as high as 166, and at any particular mass, fragments can be formed having a range of charges. There are more than 400 possible fission products of which approximately 200 have been identified.

The independent yield of a particular nuclide having mass A and charge Z is given by

$$\text{Independent Yield (\%)} = \frac{{}^{A}_{Z}N}{\text{total number of fissions}} \times 100 = {}^{A}_{Z}y$$

where ${}^{A}_{Z}N$ is the number of atoms of mass A and charge Z formed in fission, after the emission of prompt neutrons and before beta decay.

The cumulative yield of a particular mass chain A is equal to the sum of the independent yields of all the nuclides of mass A.

$$A_{Y_{cum}} = \sum_{Z} {}^{A}_{Z}y = \text{cumulative chain yield of mass A}$$

It should be noted that there are two processes which can cause the measured cumulative yield to be different from the sum of the primary yields.

(i) Delayed Neutron Emission

A few nuclides formed from beta decay emit delayed neutrons. This effect will increase the cumulative yield at mass A at the expense of the yield at mass A + 1.

(ii) Neutron Absorption

Neutron absorption by some members of a decay chain will cause a decrease in the yield of that chain, and an increase in the yield of the next higher mass chain. This effect is appreciable only for long

irradiations at high neutron flux, or for nuclides with a very high cross section.

It is possible, however, to make corrections for both these processes.

If the cumulative yields of various mass chains are plotted against the mass number, the result is a mass-yield curve. Two such curves are shown in Figure 1, for the thermal and 14-Mev neutron fission of ^{235}U. These illustrate one of the most striking features of the fission process: the most probable mode of fission is asymmetric. This double humped curve is characteristic of slow neutron fission. As the excitation energy increases, the valley between the humps fills in and the wings of the curve tend to spread out.

A closer examination of the mass-yield curve shows that it is not a completely smooth curve, but it exhibits fine structure which is most prominent in the region A = 132 - 144 and A = 90 - 100. This fine structure has been extensively studied for the fission of ^{235}U by thermal neutrons[1,2] and the fission of ^{238}U by reactor-spectrum neutrons[3]. It has not yet been definitely established whether the fine structure persists at higher excitation energies, and, accordingly, work was undertaken to determine the cumulative yields from the 14-Mev neutron fission of ^{238}U.

Using sensitive mass-spectrometric techniques, the relative yields of krypton, xenon and cesium isotopes were determined. In addition, several yields were determined by counting gross fission-product spectra using a lithium-drifted germanium (Ge(Li)) gamma-ray detector. The results indicate that the fine structure does persist at the higher excitation

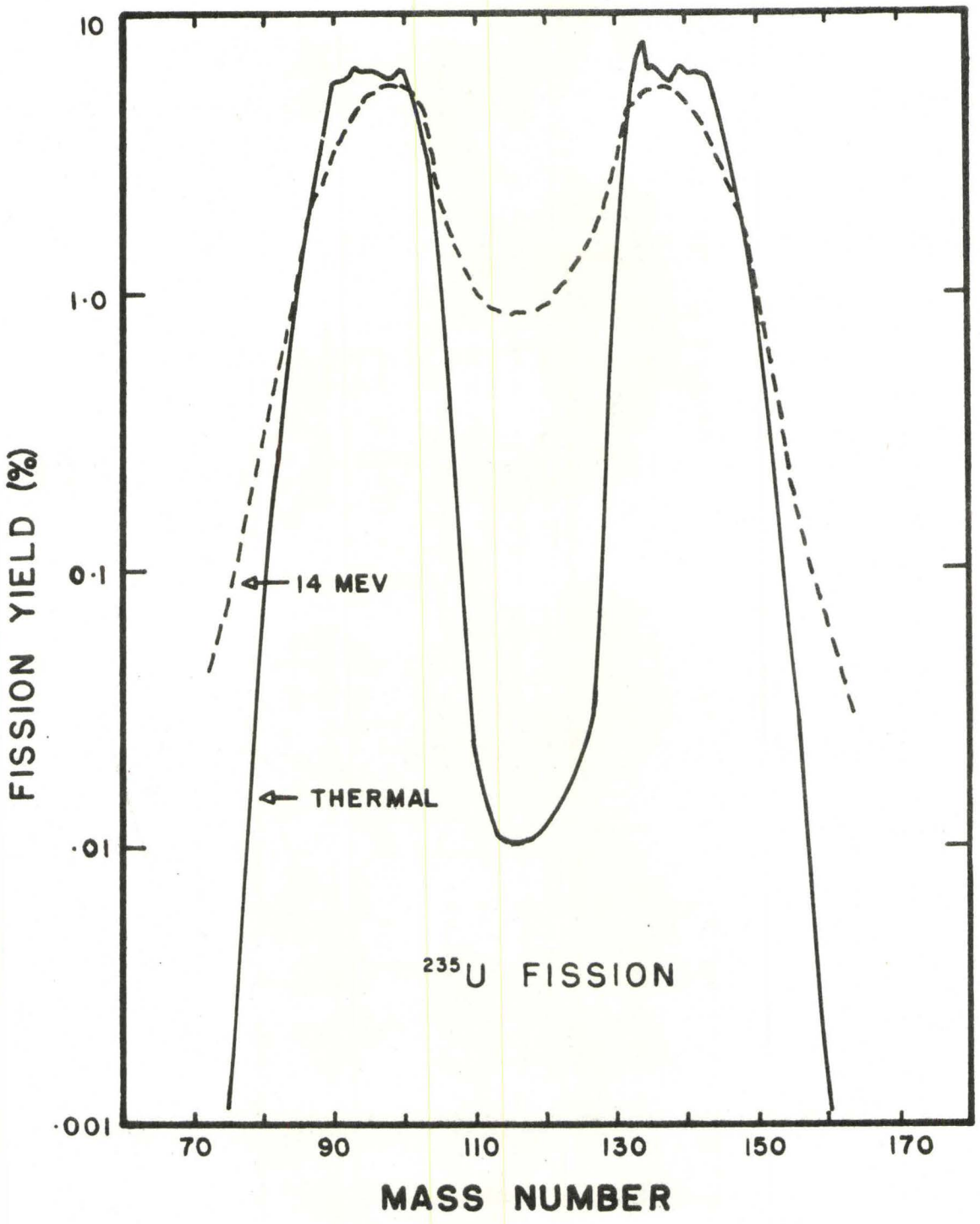

Figure 1 : Mass-Yield Curve for Thermal and 14-Mev Neutron Fission of ^{235}U (From Katcoff[22]).

energy, in particular, the peak at A = 134 is quite prominent. A semi-empirical method of obtaining the neutron-yield distribution is discussed, and, using this, a prompt-yield curve has been predicted. The prompt-yield curve for the heavy-mass distribution shows the three peaks which are typical of low-energy fission.

CHAPTER 2

HISTORICAL INTRODUCTION

A. Radiochemical Studies

Since its discovery in 1939 by Hahn and Strassmann[4], the fission process has been the object of much study. During the years 1940 - 1945, a considerable amount of work was devoted to studying the fission products from ^{239}Pu, ^{235}U, ^{238}U and ^{233}U [5]. These first fission-yield studies were limited entirely to the radiochemical method.

In the radiochemical method, a known amount of non-radioactive carrier of a given fission product element is added to a solution containing all of the fission products. After complete exchange between the radioactive and non-radioactive atoms has been attained, the desired product is separated by conventional analytic techniques in a high degree of chemical and radiochemical purity. The per cent recovery of the added carrier is determined and the same per cent recovery is assumed for the radioactive atoms. From the per cent recovery, the measured counting rate, and an estimate of the number of fissions, the fission yield is determined.

This war-time data established the general asymmetric nature of fission. The precision of the results obtained in these early studies was at best 10%, and so a smooth curve was drawn through the data to give a double humped curve which, in the case of ^{235}U gave maxima around mass numbers 96 and 138. Since 1946, better experimental techniques

have made possible the acquisition of new radiochemical data with substantially better precision. This has had particular importance in the determination of independent yields, most of which have been measured by radiochemical methods.

B. Mass Spectrometric Studies

The mass spectrometer is well suited to the measurement of fission yields. The yields of all mass chains resulting in a particular element can be determined relative to one another by measuring the isotopic ratios of that element. This can be done for several elements and the yields of different elements normalized by isotope dilution[6,7] or the isobar method.[7]

In the isotope dilution technique, the element to be analyzed is diluted with a known amount of the same element with a different isotopic composition. From a knowledge of the isotopic composition of both the sample and the diluant, the amount of the sample may be determined.

The isobar technique may be used when a decay chain has a radioactive member with a half-life long enough so that its yield may be determined relative to the other isotopes of that element; yet short enough so that it can be allowed to beta-decay to its isobar of the element one higher in charge, where its yield can again be determined relative to this element. In this way, the relative yields of the two elements can be normalized. This method requires that the decay schemes of the nuclides be known, and that their independent yields be negligible or known.

The mass spectrometer was first used to study fission products by Thode and Graham[8] in 1947. In measuring the yields of krypton

and xenon in thermal neutron fission of ^{235}U, they found that the yields of ^{134}Xe and ^{84}Kr were not consistent with a smooth mass-yield curve. Later, MacNamara, Collins, and Thode[9] showed that the yields of ^{133}Xe and ^{134}Xe were 20 and 35 per cent higher than expected on the basis of a smooth curve. This was the first evidence of a fine structure in the mass-yield curve, and further investigations with both gas-[10,11,12] and solid-source[1,7,10,12,13,14] mass spectrometry confirmed its presence.

Attempts have been made to explain this fine structure on the basis of nuclear shell effects. Glendenin[15] suggested that it was caused by an additional boil-off of neutrons from fission products with one neutron in excess of a closed shell. Pappas[16] extended this to include three, five, and seven neutrons outside a closed shell. Wiles[17] proposed that, in addition to neutron boil-off, there must be some preference in the fission act itself for the formation of fragments with a closed shell of 82 neutrons. Using the results of careful mass-spectrometric measurements of ^{235}U thermal-neutron fission yields, Farrar and Tomlinson[18] were able to explain most of the fine structure on the basis of neutron emission from the fragments.

C. Counting Techniques Using Solid-State Detectors

Using the recently developed lithium-drifted germanium detectors[19] it is possible to resolve many fission-product gamma rays which could not be resolved using the older NaI(Tl) detectors; and therefore to observe many nuclides in the gross fission-product gamma-ray spectrum without performing any chemical separations. Gordon, Harvey and Nakahara[21] studied gross fission-product gamma-ray spectra at various times after irradiation, identified about twenty fission products, and developed a

method for determining their yields.

This method is based upon the use of ^{235}U as a standard, since its fission-yields have been studied extensively and are well known[22]. Both the unknown and the ^{235}U are irradiated for the same length of time and their spectra are taken at the same time after the irradiation. By measuring the relative peak heights in the two spectra, and knowing the fission yields in the ^{235}U, the yields in the unknown can be determined. This method does not require a knowledge of the decay schemes of the fission products in order to determine the relative yields of each decay chain for which a gamma ray may be observed.

D. Summary of Work on 14-Mev Neutron Fission

To date, all of the published work on 14-Mev neutron fission yields has been done by radiochemical methods. Wahl[23] determined 14-Mev fission yields for ^{235}U in the mass region 131-135 and observed that the pronounced peak at A = 134 in thermal neutron fission is almost washed out at the higher energy. Ames et al.[24] and Cuninghame[25] reported mass yields for ^{238}U but they could not observe fine structure since in neither case were yields for more than two consecutive masses determined. Broom[26,27] determined yields for ^{238}U fission and reported fine structure at mass number 89-91 and 131-135; in addition, he also observed fine structure in the 14-MeV neutron fission of ^{232}Th [28]. James et al.[29] found evidence for fine structure in the region A = 133- 135 but this was not proven since no two adjacent masses were determined.

CHAPTER 3

EXPERIMENTAL PROCEDURE

The principal source of difficulty in this work was the extremely small sample sizes available, the limiting factor being the 14-MeV neutron flux. The neutrons were produced in a Texas Nuclear model 9509 neutron generator by the $^{3}H(d,n)^{4}He$ reaction, and the neutron flux averaged over a target lifetime of about 5 hours was approximately $5 \times 10^{7} n\,cm^{-2} sec^{-1}$. To obtain enough fission products to measure in the mass spectrometer required large samples of the order of grams and long irradiations of 20 - 30 hours. The number of fissions induced in the sample is given by

$$N_f = N_t \sigma \phi t$$

$$N_f = (5 \times 10^{8})\ wt.$$

where w is the weight of uranium in grams, and t is the length of the irradiation in hours. For 10g of uranium and an irradiation of 30 hours the number of fissions is

$$N_f = 1.5 \times 10^{11}$$

Assuming a 6% yield the number of atoms of a given fission product is about 10^{10}.

In the case of cesium, the sensitivity of the mass spectrometer is such that the minimum number of atoms required to obtain a mass spectrum

is of the order of 10^{10}, which is about the size of the sample.

The sensitivity of the mass spectrometer for the rare gases krypton and xenon is considerably higher than for cesium; hence their determination was somewhat easier and the resulting rare gas ratios are more precise than the cesium ratios.

In both cases however, because of the small sample size, contamination by the naturally occurring elements was a problem, and special precautions had to be taken to eliminate the contamination or reduce it to a tolerable level.

A. Gas Source Mass Spectrometry

(i) The Mass Spectrometer

The rare gas analyses were performed using a 10-inch radius, 90-degree sector, gas-source mass spectrometer as described by Clarke[30]. The static method was employed in which the mass spectrometer was isolated from the pumps and the sample expanded into the entire spectrometer volume[31].

(ii) Sample Preparation and Purification

The samples for the rare gas analyses consisted of approximately 5 grams of UCl_4 sealed in quartz. The UCl_4 was prepared by reacting 5 grams of metallic uranium with chlorine gas[32] in a sealed system. The apparatus is shown in Figure 2. The UCl_4 was purified by subliming it from one arm of the tube to the other while pumping on it to remove any gases. The UCl_4 was then sealed off from the vacuum system and irradiated in the neutron generator.

After irradiation and cooling, samples 1, 2 and 3 were sealed back onto a vacuum line, broken open, and the krypton and xenon separated from the UCl_4 by heating it until it sublimed. This apparatus is shown

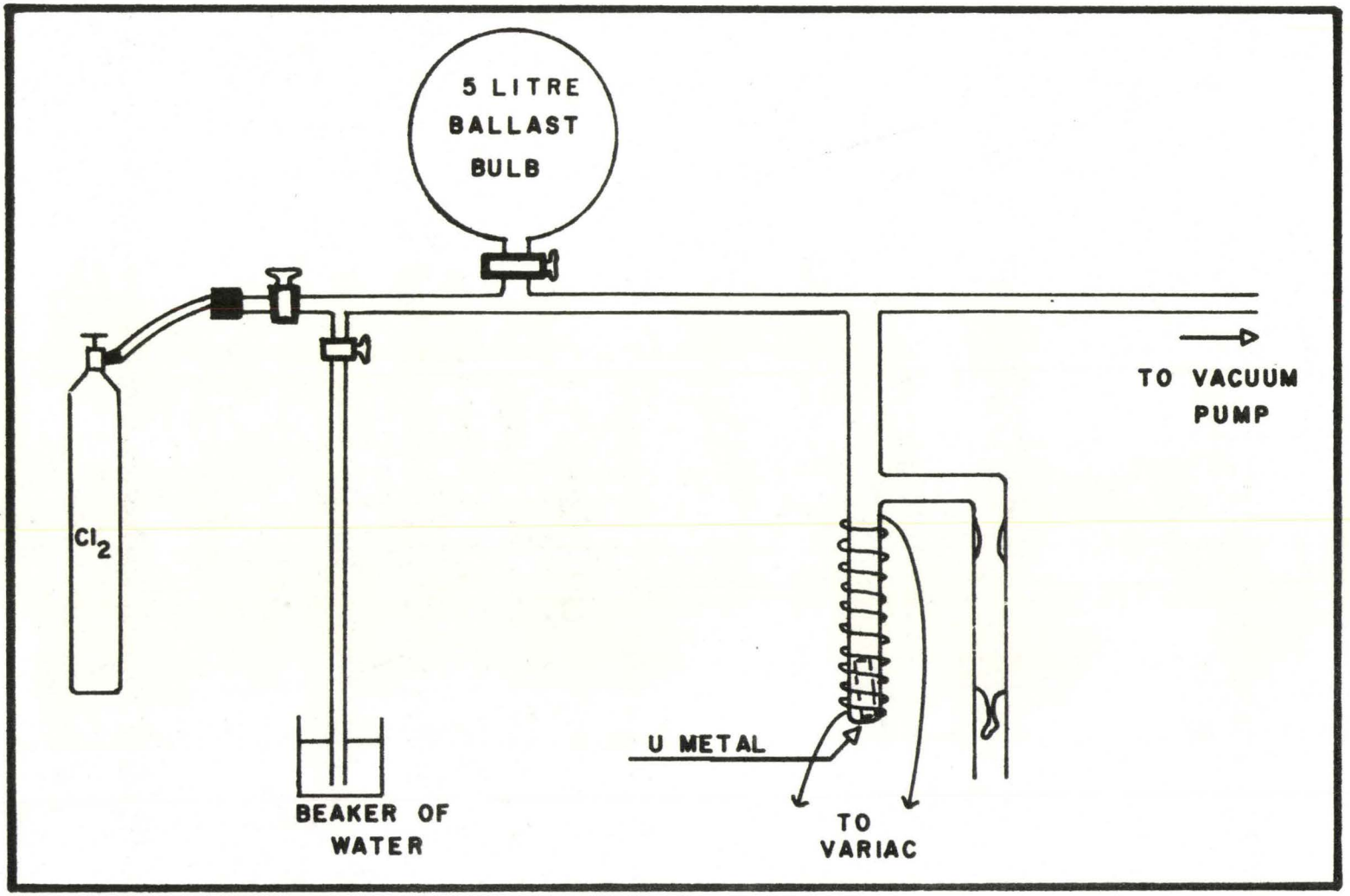

APPARATUS FOR PREPARATION OF UCl_4

Figure 2

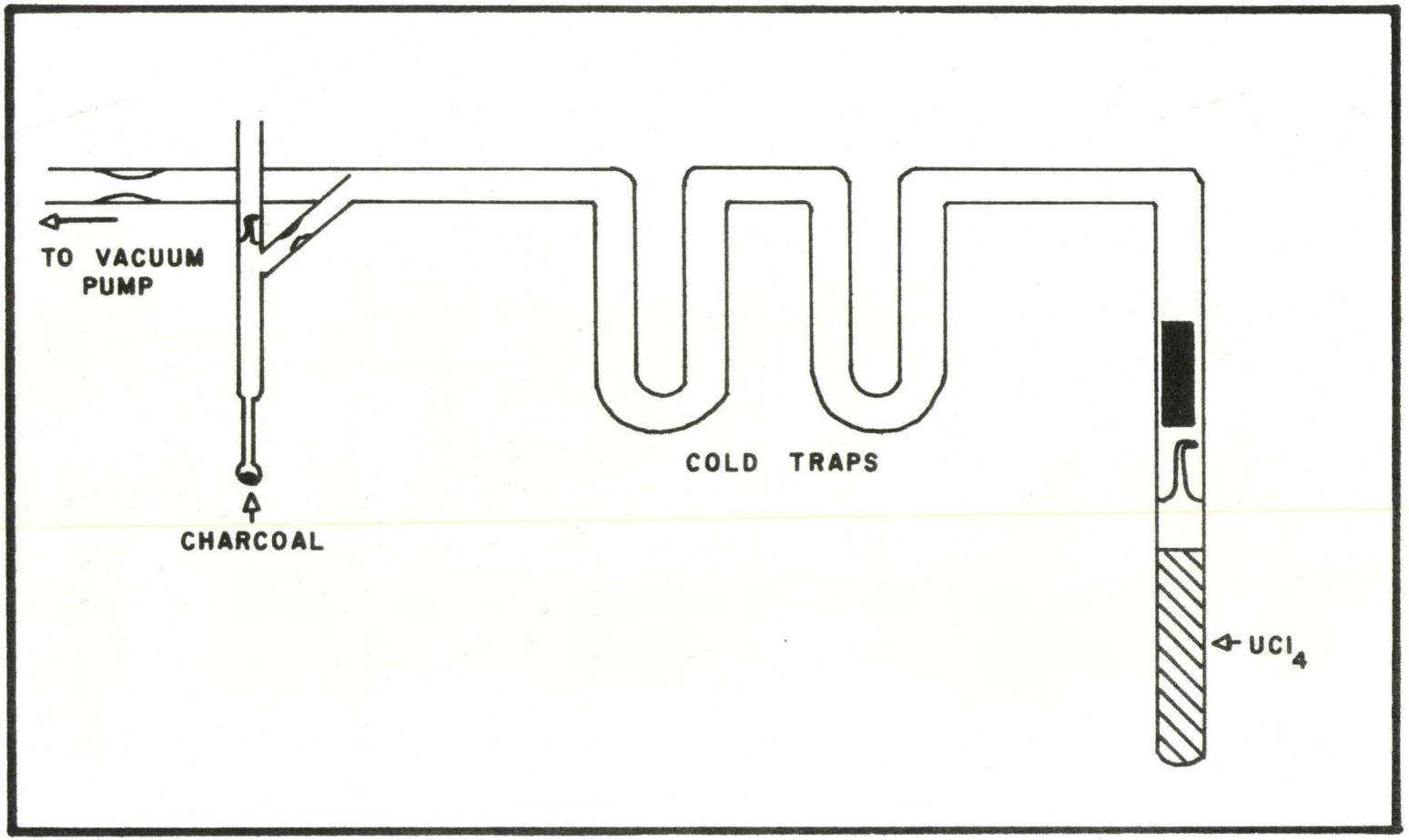

APPARATUS FOR EXTRACTION OF RARE GASES

Figure 3

in Figure 3. The rare gases were adsorbed on charcoal and transferred to the mass spectrometer for analysis. Samples 4, 5 and 6 for the determination of ^{133}Xe and ^{135}Xe were sealed directly onto the mass spectrometer, bypassing this step.

Before introducing the samples into the mass spectrometer, the gases were subjected to another purification. They were allowed to come into contact with hot titanium sponge which served as a "getter" for such impurities as nitrogen, oxygen, and chlorine. Two such purification steps were employed before admitting the sample to the mass spectrometer.

(iii) Irradiation of Samples

Samples 1, 2 and 3 were irradiated for 6 to 8 hours each day over a period of a week. They were allowed to cool for several months until all short lived precursors had decayed away. Samples 4, 5 and 6 were irradiated in one continuous irradiation and the mass spectra recorded from one to 5 days later. The irradiation data are given in Table I.

B. Solid Source Mass Spectrometry

(i) The Mass Spectrometer

The cesium ratios were obtained using a 10-inch radius, 90-degree sector, solid-source mass spectrometer with magnetic scanning and a twelve-stage electron multiplier as described by D. Irish[33].

The ion source was a multiple-filament surface-ionization type as described by Inghram and Chupka[34] with the beam centering plate omitted. The source provides for three filaments; two side filaments to hold the sample being analyzed and a centre filament to produce ions.

Table I

Irradiation Data for Samples Used to Obtain Relative Yields of Krypton and Xenon Isotopes

Sample	Irradiation Time (hours)	t_1 (hours)	t_2 (hours)
1.	23.5	+ 6100	160
2.	41.0	+ 1920	670
3.	41.0	+ 2090	450
4.	9.0	13.17	1.0
5.	9.0	118.7	1.76
6.	7.0	97.3	6.3

t_1 = time from end of irradiation to extraction of rare gases

t_2 = time from extraction of rare gases to analysis of sample

\+ an average time taken from the mid point of the series of irradiations

This arrangement allows the evaporation rate of the sample to be controlled independently of the temperature of the ionization filament. In the analyses reported here only one sample filament was used.

The nichrome source assembly was cleaned in an ultrasonic cleaner and a new set of filaments was made for each analysis. The new filaments were heated in vacuo to about 2000 degrees by passing 5-6 amps through them for 2 - 3 hours to clean the surfaces.

The filaments were made of rhenium metal ribbon .001 inches thick by .030 inches wide. During preliminary runs it was found that the tungsten filaments normally used contained cesium as an impurity in the metal. Since the sample size was very small, and the ion current produced by the cesium in the sample was of the same order of magnitude as this contamination, rhenium filaments were chosen, because they contain much less cesium than the tungsten.

(ii) Sample Preparation and Purification

In order to obtain enough cesium fission products to measure, it was necessary to prepare large samples of uranium ($\sim$ 10 grams) of extremely high purity (containing less than 10^{-12} grams of cesium). Samples were prepared using the method of peroxide precipitation[35] and anion exchange[36]. However, upon running these in the mass spectrometer, a large amount of ^{133}Cs contamination was observed. The method finally adopted was to irradiate approximately 50 g samples of uranium hexafluoride which was purified by subliming it under vacuum.

A one-pound cylinder of UF_6 was purchased from Atomergic Chemetals Company. The cylinder was connected to an all-glass vacuum line. Uranium Hexafluoride is very corrosive and it reacts with water and glass according to the following reactions[32].

$$UF_6 + 2H_2O \rightarrow UO_2F_2 + 4HF$$

$$SiO_2 + 4HF \rightarrow SiF_4 + 2H_2O$$

Consequently, it was necessary to ensure that the vacuum system was completely free of water. This was accomplished by pumping and flaming the system for three weeks prior to the introduction of the UF_6. The hexafluoride as purchased contains HF as an impurity and it was removed using the fractional-distillation procedure described by Claassen, Weinstock and Malm[37]. The purification line is shown in Figure 4.

The purification is based on the fact that at room temperature, UF_6 is a highly volatile solid with a vapour pressure of 83 mm Hg, while at dry-ice temperature (- 78.5°C) its vapour pressure is of the order of 10^{-6} mm and that of HF is several mm Hg [37,38].

Care must be taken when condensing UF_6 at low temperature. The hexafluoride has a very large coefficient of expansion and if it is condensed on a concave surface at low temperature and allowed to warm up it may expand and break the glass[39]. For this reason the UF_6 is condensed on convex surfaces in traps B and C in Figure 4.

After closing the system off from the pumps by sealing constriction 1, the UF_6 was removed from the cylinder and condensed in trap A by placing trap A in ice water and holding the cylinder at room temperature to minimize the contribution of volatile impurities. Only a small amount of UF_6 was brought over at a time, where it condensed on the walls. The tube was then warmed up and the UF_6 crystals flaked off the walls and fell to the bottom of the tube. The procedure was repeated until about 50 grams of UF_6 were brought over.

At this point a mixture of dry-ice acetone was placed in the

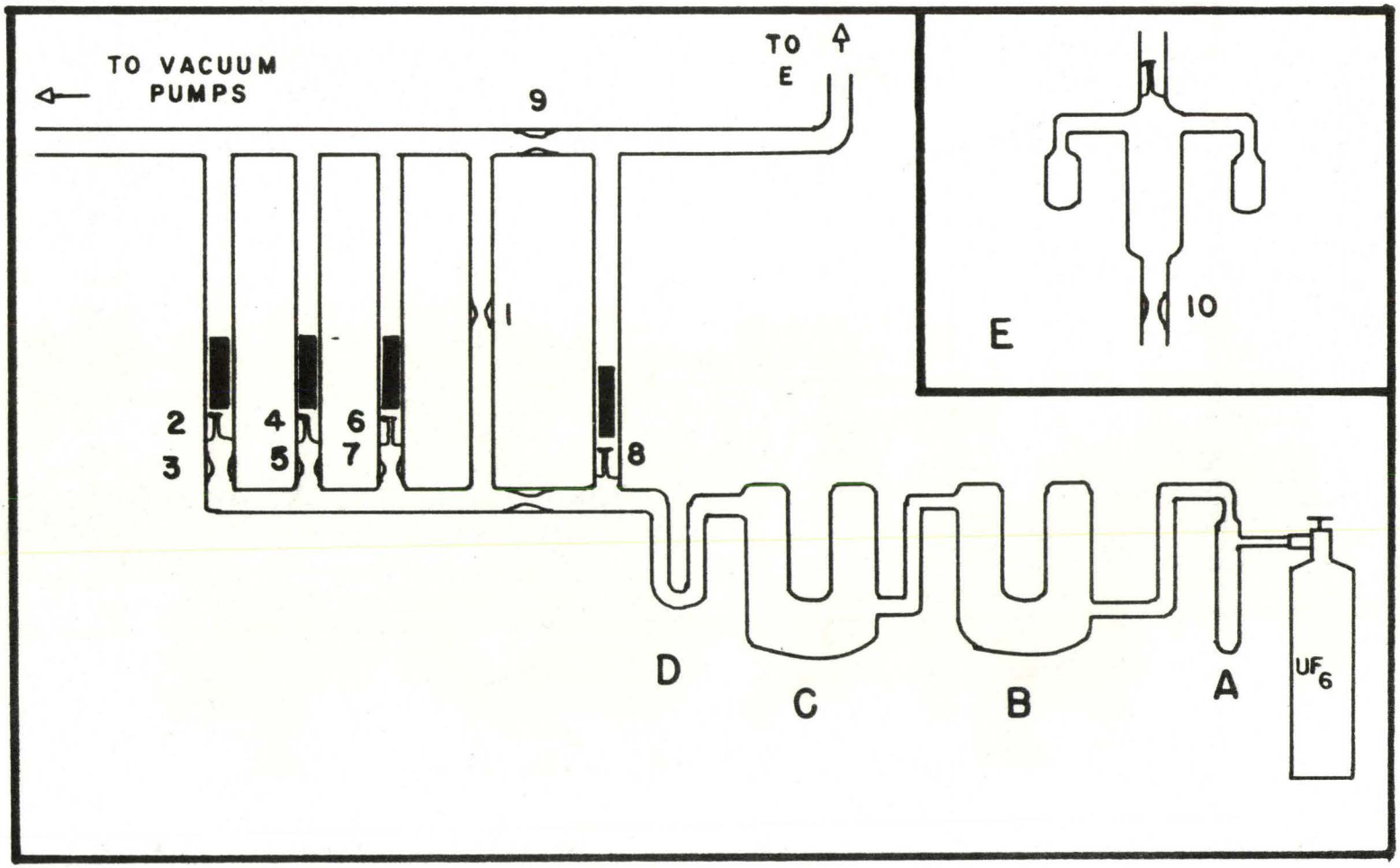

Figure 4 - UF_6 PURIFICATION LINE

A - ice-water cooled condensing trap
B,C,D - dry-ice acetone cooled traps
E - purified UF_6 collection vessel
2,4,6,8 - breakseals
1,3,5,7,9,10 - contrictions

reentrant tube in trap B, breakseal 2 was broken to open the system to the pumps, and the UF_6 was allowed to distill from trap A to trap B while pumping was continued. In a second purification step, this process was repeated as the UF_6 was distilled from trap B to trap C.

The final purified UF_6 was collected in bulb E by keeping it at 0°C and the rest of the line at room temperature. The final receptacle was then sealed off from the vacuum line and irradiated.

Before running the irradiated sample in the mass spectrometer the uranium hexafluoride was separated from the fission products by distilling it into another receptacle. The non-volatile fission products remained behind on the walls of the tube, and they were dissolved in a small amount of dilute HCl. The pure HCl was prepared by dissolving HCl gas in water which had been purified by passage through a mixed-bed ion-exchange column of Dowex-1 and Dowex-50, followed by a second passage through a cation-exchange column of Dowex 50W - X8. The solution was evaporated down to one drop under an infra-red lamp and then applied directly to the filament of the mass spectrometer.

(iii) Irradiation of Samples

The UF_6 samples were irradiated for 6 - 8 hours each day over a period of 1 week. They were allowed to cool for several months before the mass spectra were determined. The irradiation data are given in Table II.

C. Ge(Li) Spectrometry

(i) Description of Equipment

The detector used was an ORTEC model 8145 lithium-drifted germanium detector with a volume of 2 cm^3. The pulses were amplified with an ORTEC model 118A FET preamplifier and a model 410 linear amplifier.

Table II

Irradiation Data for Cesium

Sample	Total Length of Irradiation	Time from Irradiation to Analysis*
1.	23.5 h	71 d
2.	41.0 h	101 d

* an approximate time taken from the mid-point of the series of irradiations.

The full-width at half-maximum of the 662-keV ^{137}Cs line was about 3.4 kev. Pulses were analyzed and stored in a Nuclear Data 4096 channel pulse height analyzer. Readout from the analyzer was by means of a Potter MT-24 magnetic tape unit.

(ii) Sample Preparation, Irradiation, and Counting

Like the mass-spectrometric measurements, the counting method also was limited by the low 14-Mev neutron flux available. Because the fission cross section of ^{238}U (1.17b)[56] is comparable to the (n,2n) cross section (880 mb),[55] ^{237}U was produced in approximately the same yield as the fission products. The ^{237}U has a number of gamma rays with energies less than 100 keV and these completely obscured any fission-product gamma rays below this energy, in particular, the 91.1-keV gamma ray from ^{147}Nd. Furthermore, since the uranium has such a high atomic number, low-energy gamma rays are severely attenuated, and, in order to avoid absorption corrections, the ^{238}U sample and the ^{235}U standard must be identical. This necessitated irradiating natural uranium for both the ^{238}U unknown and the ^{235}U standard.

Three identical samples of natural uranium foil weighing 80 mg each were sealed in a 0.5 mm. thick polyethylene packet. These constituted samples A, B, and C. Sample A was irradiated in the thermal column of the McMaster reactor for 5 hours at a thermal neutron flux of approximately 10^8 n cm^{-2} $sec.^{-1}$. Under these conditions, only the ^{235}U in the sample undergoes fission; therefore, sample A was used as the ^{235}U standard. Samples B and C were irradiated in a 14-Mev neutron flux of $\sim 10^8$ n cm^{-2} $sec.^{-1}$ from the neutron generator. Since these samples contain 99.27% ^{238}U, and since the 14-Mev fission cross sections of ^{238}U and ^{235}U are comparable, essentially all of the fissions are from ^{238}U.

Gross fission-product gamma-ray spectra were obtained for samples A, B, and C at 3, 5, 6, 18 and 24 hours after the end of irradiation, with the samples still sealed in polyethylene. Thereafter spectra were recorded once a day for the first week and every two or three days for the next two weeks.

In order to obtain the yield of ^{147}Nd it was necessary to separate it from the uranium after the irradiation. To accomplish this another set of samples was prepared. Sample D was used as a standard and it consisted of 2 mg of U_3O_8 enriched to 93.18% in ^{235}U. This was sealed in a quartz capsule and irradiated in the McMaster reactor for one hour at a flux of $\sim 10^8$ n cm^{-2} $sec.^{-1}$. Samples E and F consisted of about 1 gram of reagent-grade uranyl nitrate sealed in a polyethylene capsule. The uranyl nitrate was purified by adsorbing the uranium on Dowex AG1 - X8 anion exchange resin in 9M HCl solution. Under these conditions the rare earths are not adsorbed.[36]

These samples were irradiated with 14-Mev neutrons for 1 hour.

Approximately 12 hours after the irradiation samples D, E, and F were broken open, dissolved in 9M HCl and a mixture of rare earths added as a carrier . The uranium was adsorbed on Dowex AG1 - X8 anion exchange resin[36]. Both uranium and rare-earth fractions were evaporated to dryness and spectra were taken of each. In samples D, E, and F, spectra were recorded once a day for five days after the irradiation.

The composition of these samples and the irradiation data are summarized in Table III.

TABLE III

Irradiation Data for Samples Used
in Counting Experiments

Sample	Neutron Energy	Type of Fission	Duration of Irradiation (hours)
A	Thermal	^{235}U	5
B	14 - MeV	^{238}U	5
C	14 - MeV	^{238}U	5
D	Thermal	^{235}U	1
E	14 - MeV	^{238}U	1
F	14 - MeV	^{238}U	1

In all cases, the neutron flux was approximately 10^{8} n cm^{-2} sec^{-1}

CHAPTER 4

EXPERIMENTAL RESULTS AND TREATMENT OF DATA

A. Krypton

(i) Correction for Contamination

The isotopic abundances of fission-product krypton measured relative to mass 86 are shown in Table V. It was necessary to correct these ratios for contamination by atmospheric krypton. The extent of contamination was determined from the measured ^{80}Kr and ^{82}Kr which do not occur as fission products. However, it was found that the $^{80}Kr/^{82}Kr$ ratio was not that of natural krypton and that this ratio varied from sample to sample. The ratios are given in Table IV.

If the observed ratios are corrected for natural contamination assuming that the ^{82}Kr consists entirely of natural krypton, the resulting ratios from the three samples do not agree within the statistical errors. This can be seen in Table V. The agreement is poorest for ^{84}Kr which is the isotope most affected by the correction, since it forms 56.9% of atmospheric krypton.

In order to account for the mass 80/82 ratio, it was assumed that, in addition to natural krypton, there was some other impurity present having a 80/82 ratio (R) which did not vary from sample to sample. Krypton ratios were then computed for different values of this ratio in the range $0 \leq R \leq \infty$. It was found that the results from the three samples were most consistent when the ratio was in the range $0.9 \leq R \leq 1.20$. Using

Table IV

Measured $^{80}Kr/^{82}Kr$ Ratios

Sample	^{80}Kr	^{82}Kr
1.	0.438	1.000
2.	0.218	1.000
3.	0.341	1.000
atmosphere	0.196	1.000

Table V

Relative Yields of Krypton Isotopes

	Sample	Relative Abundances					
		80	82	83	84	85	86
1.	Measured Ratio	0.0616	0.1407	0.4588	1.1173	0.1189	1.000
	Relative Yield (a)			0.4033	0.5378	0.1507	1.000
	(b)			0.4225	0.7382	0.1398	1.000
	(c)			0.423	0.738	0.652	1.000
	Standard Deviation			0.007	0.020	0.015	
2.	Measured Ratio	0.0330	0.1502	0.4642	1.281	0.1030	1.000
	Relative Yield (a)			0.4017	0.6946	0.1329	1.000
	(b)			0.4076	0.7209	0.1320	1.000
	(c)			0.408	0.721	0.598	1.000
	Standard Deviation			0.017	0.022	0.014	
3.	Measured Ratio	0.0274	0.0803	0.4489	0.9674	0.1295	1.000
	Relative Yield (a)			0.4190	0.6492	0.1473	1.000
	(b)			0.4250	0.7163	0.1438	1.000
	(c)			0.425	0.716	0.640	1.000
	Standard Deviation			0.006	0.008	0.007	
	Average			0.423	0.716	0.635	1.000
	Standard Deviation			0.004	0.007	0.006	

(a) Ratio corrected assuming that mass 82 is 100% natural krypton.

(b) Ratio corrected assuming that masses 80 and 82 are a mixture of atmospheric krypton and HBr.

(c) Krypton-85 corrected for decay assuming a 10.60y half life for Kr-85 and assuming that 22.5% of the 4.4h isomer decays to the ground state of krypton.[48]

the 84/86 ratio, which is most sensitive to the correction, the best value of R in the least-squares sense was R = 1.12.

The most likely contaminant is HBr, which is known to be present as a background in the mass spectrometer and which would give an 80/82 ratio of 1.02[48]. Further evidence that this is background is seen in the fact that the correction was smallest for the samples which were irradiated for the longest time (Table III) i.e., for the samples with the largest amount of fission products.

Accordingly, the reported krypton yields are corrected on the basis of contamination by HBr assuming that the measured 80/82 ratio is made up of atmospheric krypton with an 80/82 ratio of 0.196 and HBr with an 80/82 ratio of 1.02.

(ii) Correction for Decay and Branching in ^{85}Kr

The ^{85}Kr yield must be corrected for decay of the isomer ^{85m}Kr whose decay scheme is as follows:[48]

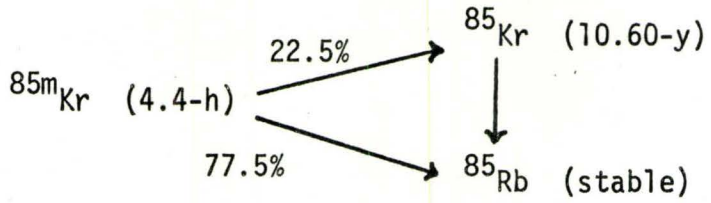

The krypton ratios were measured after all of the ^{85m}Kr had decayed, therefore there were two corrections applied to the ^{85}Kr.

(1) a correction for decay of the ^{85}Kr

(2) a correction for the amount (77.5%) of the ^{85m}Kr which decayed directly to ^{85}Rb.

The assumption was made that the independent yield of ^{85m}Kr is zero. This is a reasonable assumption since a calculation using the Equal Charge Displacement (ECD) method[40] gives an independent yield

for ^{85}Kr of only 0.03% of the chain.

The cumulative yield of the A = 85 mass chain is thus given by

$$y_{85} = [^{85}Kr]_{meas}\, e^{\lambda(t-t_o)} + \frac{77.5}{22.5}[^{85}Kr]_{meas}\, e^{\lambda(t-t_o)}$$

$$= \frac{100}{22.5}[^{85}Kr]_{meas}\, e^{\lambda(t-t_o)}$$

$$= 4.444\,[^{85}Kr]_{meas}\, e^{\lambda(t-t_o)} \qquad (4\text{-}1)$$

$\lambda = 1.79 \times 10^{-4}\ d^{-1}$ assuming half-life of 10.60 y for ^{85}Kr.[48] The final corrected ratios are given in Table V.

B. Xenon

(i) Correction for Contamination

The xenon ratios were corrected for contamination by atmospheric xenon by assuming that the measured ^{129}Xe was 100% atmospheric xenon.

(ii) Correction for Decay and Branching in 133 and 135 Mass Chains

The yields of ^{133}Xe and ^{135}Xe were corrected for decay and hold-up in the isomeric state. Their decay schemes are as follows:[48]

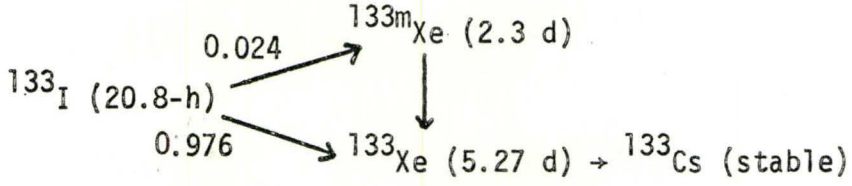

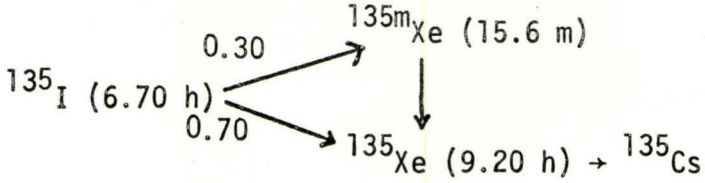

The differential equations of radioactive growth and decay are similar for the two chains and they have the following form for times during the irradiation.

$$\frac{dN_1}{dt} = R_1 - N_1\lambda_1 \qquad (4\text{-}2)$$

$$\frac{dN_2}{dt} = R_2 + aN_1\lambda_1 - N_2\lambda_2 \qquad (4\text{-}3)$$

$$\frac{dN_3}{dt} = R_3 + bN_1\lambda_1 + N_2\lambda_2 - N_3\lambda_3 \qquad (4\text{-}4)$$

Here, R_1 is the rate of production of N_1 during the irradiation and R_2 and R_3 are the rates of production of N_2 and N_3 independently during the irradiation. N_1 is ^{133}I or ^{135}I, N_2 is ^{133m}Xe or ^{135m}Xe, and N_3 is ^{133}Xe or ^{135}Xe. The constants a and b are the branching ratios for the iodine. For the 133 mass chain a = 0.024, b = 0.976. For the 135 mass chain a = 0.30, b = 0.70.[48]

These equations have the following solution (derived in Appendix B) for N_1, N_2 and N_3 at any time t after the end of the irradiation.

$$N_1 = \frac{R_1}{\lambda_1}\left[1 - e^{-\lambda_1 T}\right] e^{-\lambda_1 t} \qquad (4\text{-}5)$$

$$N_2 = N_2^* e^{-\lambda_2 t_2} \qquad (4\text{-}6)$$

$$N_3 = N_3^* e^{-\lambda_3 t_2} + N_2^* \frac{\lambda_2}{\lambda_3 - \lambda_2}\left[e^{-\lambda_2 t_2} - e^{-\lambda_3 t_2}\right] \qquad (4\text{-}7)$$

$$N_2^* = aR_1\left[\frac{(1 - e^{-\lambda_1 T})}{\lambda_2 - \lambda_1} e^{-\lambda_1 t_1} - \frac{\lambda_1(1 - e^{-\lambda_2 T})}{\lambda_2(\lambda_2 - \lambda_1)} e^{-\lambda_2 t_1}\right] + \frac{R_2}{\lambda_2}(1 - e^{-\lambda_2 T}) e^{-\lambda_2 t_1} \qquad (4\text{-}8)$$

$$N_3^* = aR_1 \left[\frac{\lambda_2(1 - e^{-\lambda_1 T})}{(\lambda_2-\lambda_1)(\lambda_3-\lambda_1)} e^{-\lambda_1 t_1} - \frac{\lambda_1(1 - e^{-\lambda_2 T})}{(\lambda_2-\lambda_1)(\lambda_3-\lambda_2)} e^{-\lambda_2 t_1} \right.$$

$$\left. + \left(\frac{1}{\lambda_3} + \frac{\lambda_1}{(\lambda_2-\lambda_1)(\lambda_3-\lambda_2)} - \frac{\lambda_2}{(\lambda_2-\lambda_1)(\lambda_3-\lambda_1)}\right)(1 - e^{-\lambda_3 T}) e^{-\lambda_3 t_1} \right]$$

$$+ bR_1 \left[\frac{(1 - e^{-\lambda_1 T})}{\lambda_3 - \lambda_1} e^{-\lambda_1 t_1} - \frac{\lambda_1(1 - e^{-\lambda_3 T})}{\lambda_3(\lambda_3 - \lambda_1)} e^{-\lambda_3 t_1} \right]$$

$$+ R_2 \left[\frac{(1 - e^{-\lambda_2 T})}{\lambda_3 - \lambda_2} e^{-\lambda_2 t_1} - \frac{\lambda_2(1 - e^{-\lambda_3 T})}{\lambda_3(\lambda_3 - \lambda_2)} e^{-\lambda_3 t_1} \right]$$

$$+ R_3 \left[\frac{1}{\lambda_3} (1 - e^{-\lambda_3 T}) e^{-\lambda_3 t_1} \right] \qquad (4\text{-}9)$$

Here, T is the length of the irradiation, t_1 is the time from the end of the irradiation to the separation of the xenon from the iodine precursor, and t_2 is the time from the separation from the iodine to the determination of the ratios.

A calculation of the independent yield of ^{133}Xe by the ECD method[40] gives a fractional chain yield of .008%. This is small enough that it can be neglected, and therefore for the 133 mass chain, $R_2 = R_3 = 0$.

In the case of the ^{135}Xe, however, the independent yield is not negligible. This yield has been calculated using the ECD method[40] and the displacement method of Coryell[41] and an average value of $3.0 \pm 1.5\%$ has been used in correcting for it. The calculations leading to this value are given in Appendix C. The correction is not sensitive to the ratio R_2/R_3 ; the yield of ^{135}Xe remains within the given errors

for all values of this ratio from zero to infinity.

The relative yields of the Xenon isotopes are given in Table VI.

C. Cesium

(i) Correction for Natural Contamination

In spite of the precautions taken to purify the uranium, the cesium samples were found to contain a large amount of ^{133}Cs contamination relative to the size of the sample, which was of the order of 10^9 - 10^{10} atoms of cesium. Because this contamination was 10^3 - 10^4 times the amount of ^{135}Cs and ^{137}Cs, it was not possible to measure any fission product ^{133}Cs. Such small samples lie on the lower limits of detection by mass spectrometry; the smallest sample of cesium that has been measured was 10^8 atoms of ^{132}Cs and ^{134}Cs in the presence of 10^4 times as much ^{133}Cs.(47) In addition, the ^{135}Cs and ^{137}Cs were contaminated with natural barium from the ion source filaments. It was possible to correct for this by using the measured ^{138}Ba and the known natural abundances of the barium isotopes.

(ii) Correction for Decay of ^{137}Cs

The ^{137}Cs is corrected for decay assuming a half-life of 30.4 y.(48). The final cesium ratios are shown in Table VII.

D. Results from Gamma-Ray Spectrometry

Some sample spectra which were obtained are shown in Figures 5 to 11; the observed nuclides and the energies of their gamma rays are given in Table VIII which is reproduced from reference 21 with some additions. The ^{235}U spectra show peaks from ^{239}Np which is produced by an (n,γ) reaction on the ^{238}U in the sample. One ^{239}Np peak at 228 keV coincides with the ^{132}Te peak; however, since the A=132 yield was obtained from ^{132}I and from mass spectrometry it was not considered necessary to

Table VI

Relative Yields of Xenon Isotopes

Sample	Relative Abundance							
	129	130	131	132	133	134	135	136
1. Measured Ratio	0.9827		1.1679	1.4816		1.000		0.8731
Relative Yield (a)			0.622	0.782		1.000		0.888
Standard Deviation			0.008	0.012				0.009
2. Measured Ratio	0.0237	0.004666	0.6317	0.7766		1.000		0.8793
Relative Yield (a)		0.00102	0.618	0.759		1.000		0.880
Standard Deivation		0.00003	0.003	0.005				0.005
3. Measured Ratio	0.3315	0.0560	0.7980	0.9945		1.000		0.8846
Relative Yield (a)		0.00098	0.612	0.756		1.000		0.891
Standard Deviation		0.00036	0.006	0.006				0.010
4. Measured ratio	0.01413				0.3880	1.000	0.3149	0.8825
Relative Yield (a)					0.3902	1.000	0.3174	0.8820
(b)					0.934	1.000	0.906	0.882
Standard Deviation					0.001	1.000	.016	0.005

continued . . .

Table VI (continued)

Relative Yields of Xenon Isotopes

Sample		Relative Abundance							
		129	130	131	132	133	134	135[t]	136
5.*	Measured Ratio	0.0521				0.5638	1.000		
	Relative Yield (a)					0.5744	1.000		
	(b)					0.987			
	Standard Deviation					0.009			
6.	Measured Ratio	0.0254	0.0505			0.5925	1.000		0.8861
	Relative Yield (a)		0.00115			0.5978	1.000		0.8867
	(b)		0.00115			0.948	1.000		0.887
	Standard Deviation		0.00005			0.014			0.007
	Average			0.618	0.760	0.935	1.000	0.906	0.883
	Standard Deviation			0.002	0.004	0.001		0.016	0.003

(a) Ratio corrected assuming that mass 129 is 100% natural xenon.

(b) Ratio corrected for hold-up in isomeric state and independent yield of xenon.

* Sample discarded due to large hydrocarbon contamination

t Assuming independent yield of Xe^{135} is 3.0 $\pm$ 1.5% of chain.

Table VII

Relative Yields of Cesium Isotopes

Sample		Relative Abundance 135	137
1.	Measured Ratio	1.00	0.860
	Relative Yield (a)	1.00	0.860
	(b)	1.00	0.863
	Standard Deviation		0.116
2.	Measured Ratio	1.00	0.936
	Relative Yield (a)	1.00	0.858
	(b)	1.00	0.863
	Standard Deviation		0.130
	Average	1.00	0.863
	Standard Deviation		0.086

(a) Ratio corrected for natural Barium contamination

(b) Ratio corrected assuming a half-life for Cs-137 of 30.4 y. [48]

Table VIII

Prominent Gamma Rays Observed from Fission Products
(reproduced from reference (21))

Nuclide	Energy of peaks analyzed (keV)	Time analyzed after end of irradiation
4.4 -hr. ^{85m}Kr	151.1	first day
9.7 -hr. ^{91}Sr-51-min ^{91m}Y	555.7	first two days
65 -day ^{95}Zr - 35-day ^{95}Nb*	724.5, 757.2; 766.2	after ten days
17 -hr. ^{97}Zr - 73-min ^{97}Nb	743.5; 658.0	first three days
67 -hr. ^{99}Mo - 6.0-hr. ^{99m}Tc	140.5	first two weeks
40 -day ^{103}Ru	497.4	after ten days
8.05-day ^{131}I	364.5	after five days
78 -hr. ^{132}Te - 2.3-hr. ^{132}I	228.2; 667.8, 772.8	first two weeks
20.8-hr. ^{133}I - 5.3-day ^{133}Xe	529.9	first three days; after two weeks
9.2 -hr. ^{135}Xe	249.7	first three days
82 -min. ^{139}Ba	165.8	first day
12.8-day ^{140}Ba - 40-hr. ^{140}La	537.4; 487.3	after five days
33 -day ^{141}Ce†	145.6	after ten days
33 -hr. ^{143}Ce†	293.3	first five days
284 -day ^{144}Ce*	133.3	after one month
11.1-day ^{147}Nd†	91.1	after two weeks
2.35-day ^{239}Np	209.4, 228.2, 277.5 316.2, 334.8	after two weeks
6.75-day ^{237}U	207.5	

* not observed in ^{238}U spectra because of low activity of sample

† separated from uranium and measured first five days after irradiation

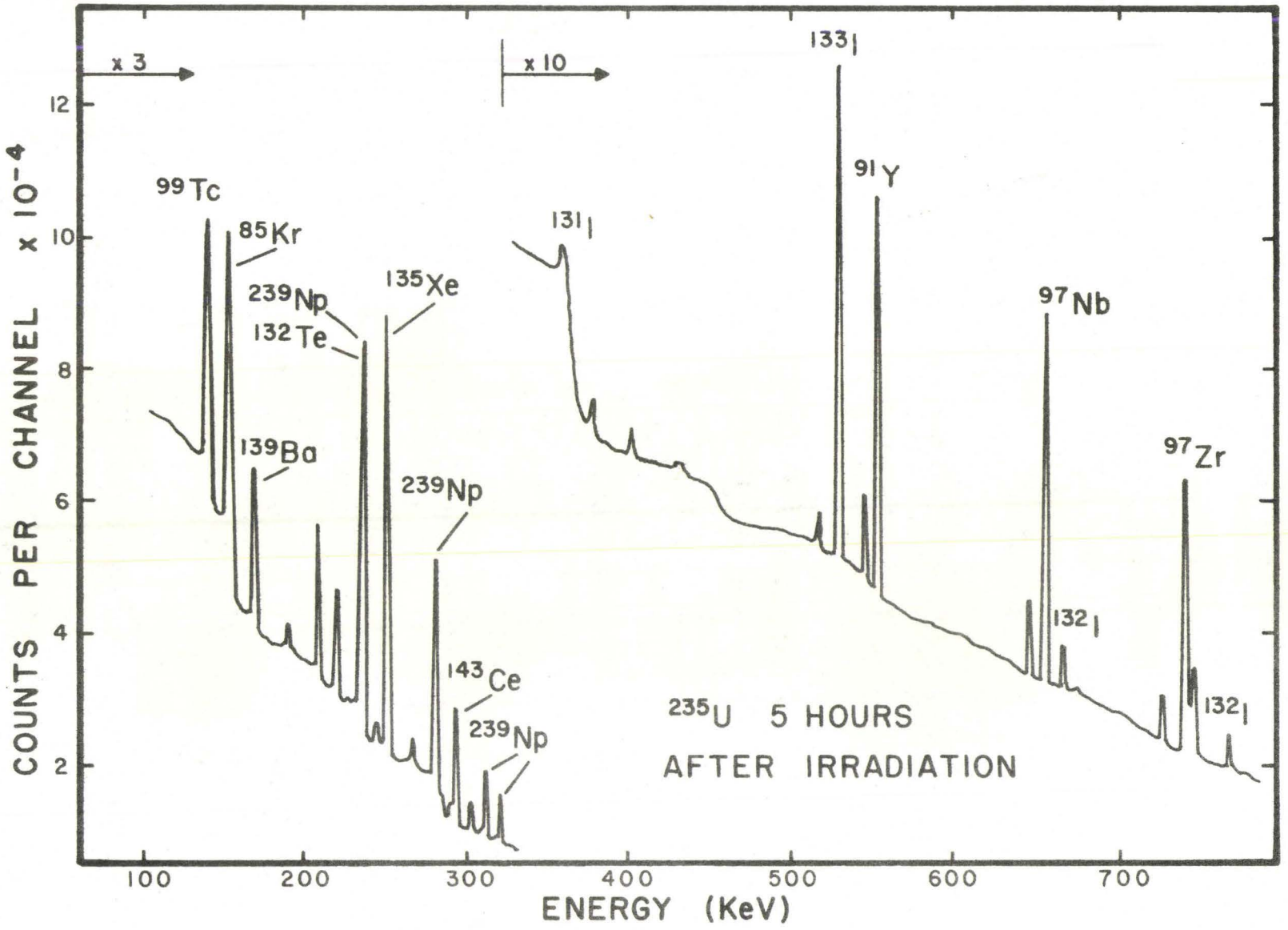
x 3
x 10
133I
91Y
131I
99Tc
85Kr
239Np
132Te
135Xe
97Nb
139Ba
239Np
97Zr
132I
143Ce
239Np
132I
235U 5 HOURS
AFTER IRRADIATION
COUNTS PER CHANNEL x 10-4
ENERGY (KeV)
2
4
6
8
10
12
100
200
300
400
500
600
700

Figure 5

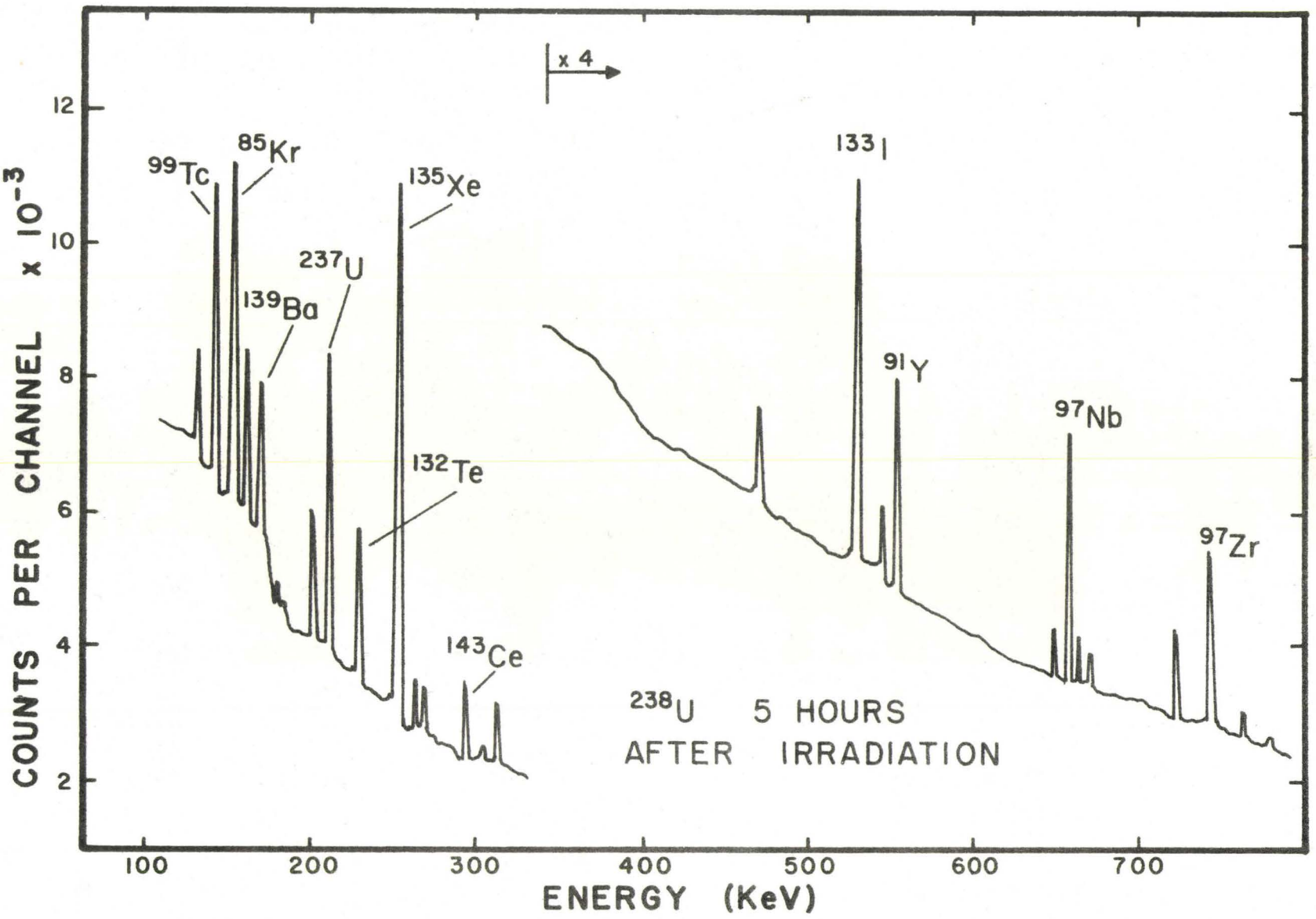
x 4
99Tc
85Kr
139Ba
237U
135Xe
132Te
143Ce
133I
91Y
97Nb
97Zr
238U 5 HOURS
AFTER IRRADIATION
COUNTS PER CHANNEL x 10-3
ENERGY (KeV)
2
4
6
8
10
12
100
200
300
400
500
600
700

Figure 6

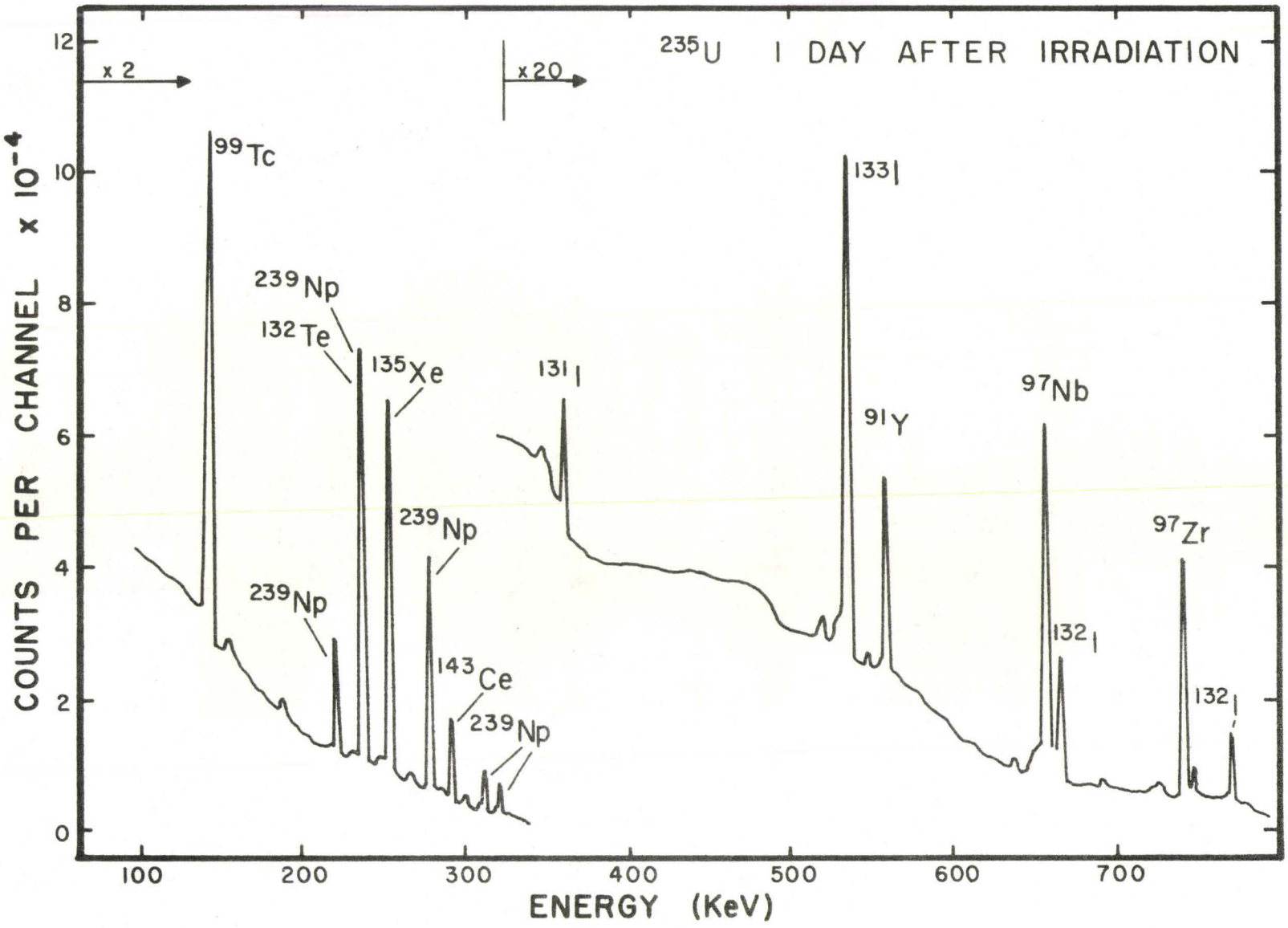
235U 1 DAY AFTER IRRADIATION
x 2
x 20
99Tc
239Np
132Te
135Xe
239Np
239Np
143Ce
239Np
131I
133I
91Y
97Nb
132I
97Zr
132I
COUNTS PER CHANNEL x 10-4
ENERGY (KeV)
0
2
4
6
8
10
12
100
200
300
400
500
600
700

Figure 7

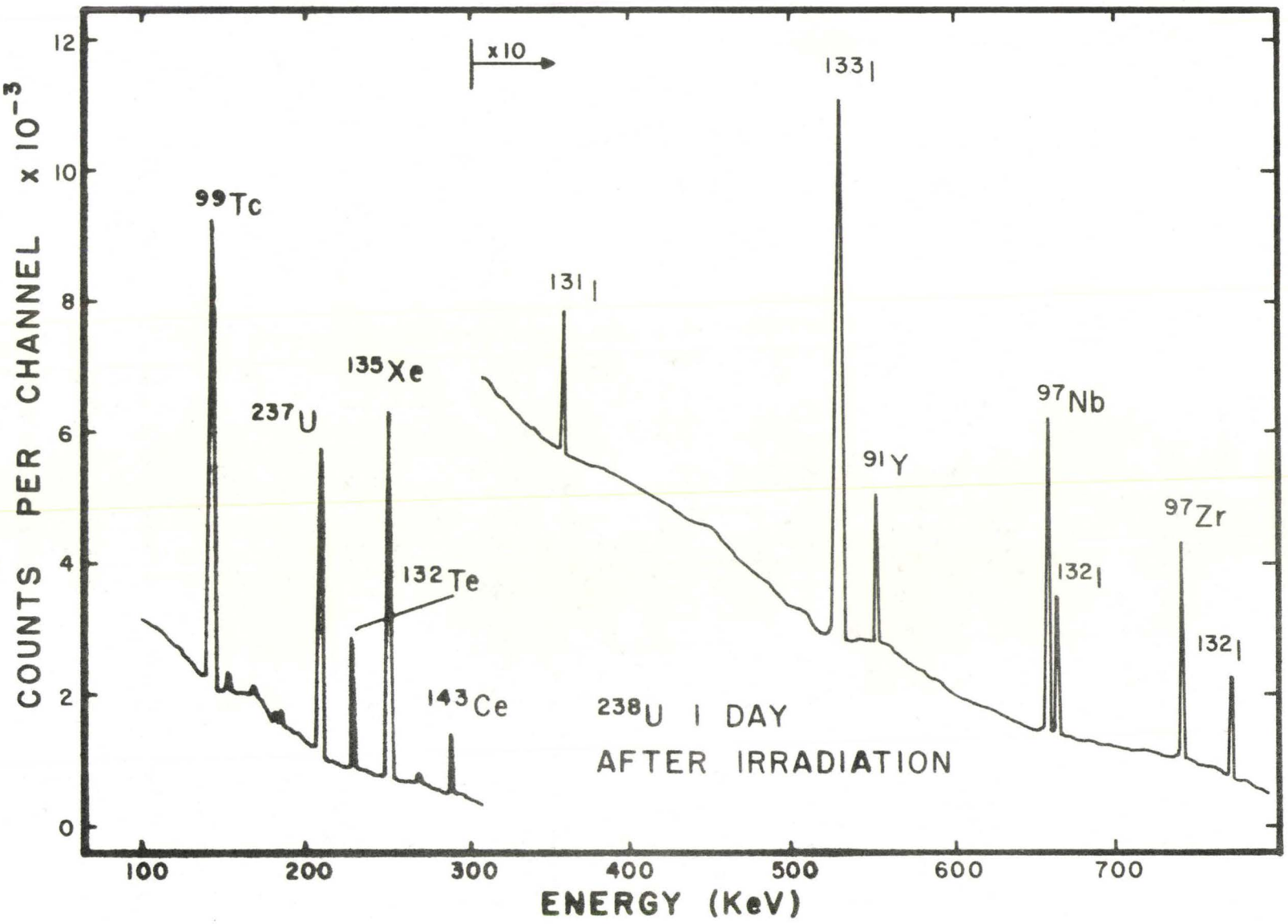
COUNTS PER CHANNEL x 10⁻³
ENERGY (KeV)
x10
99Tc
237U
135Xe
132Te
143Ce
131I
133I
91Y
97Nb
132I
97Zr
132I
238U 1 DAY
AFTER IRRADIATION

Figure 8

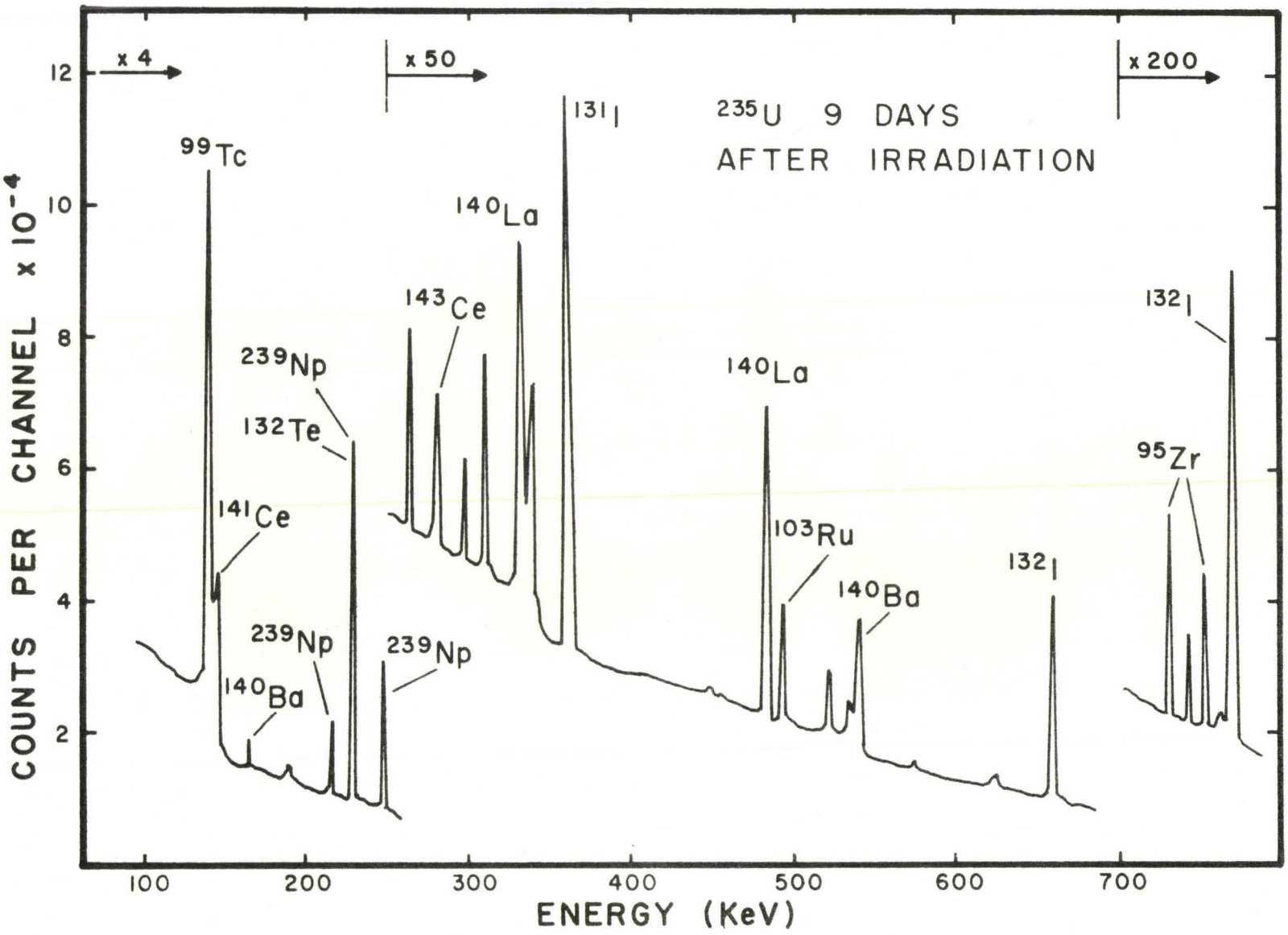
x 4
x 50
x 200
^{235}U 9 DAYS
AFTER IRRADIATION
^{99}Tc
^{131}I
^{140}La
^{143}Ce
^{239}Np
^{132}Te
^{141}Ce
^{140}La
^{132}I
^{95}Zr
^{103}Ru
^{140}Ba
^{132}I
^{239}Np
^{140}Ba
^{239}Np
COUNTS PER CHANNEL x 10^{-4}
ENERGY (KeV)
2
4
6
8
10
12
100
200
300
400
500
600
700

Figure 9

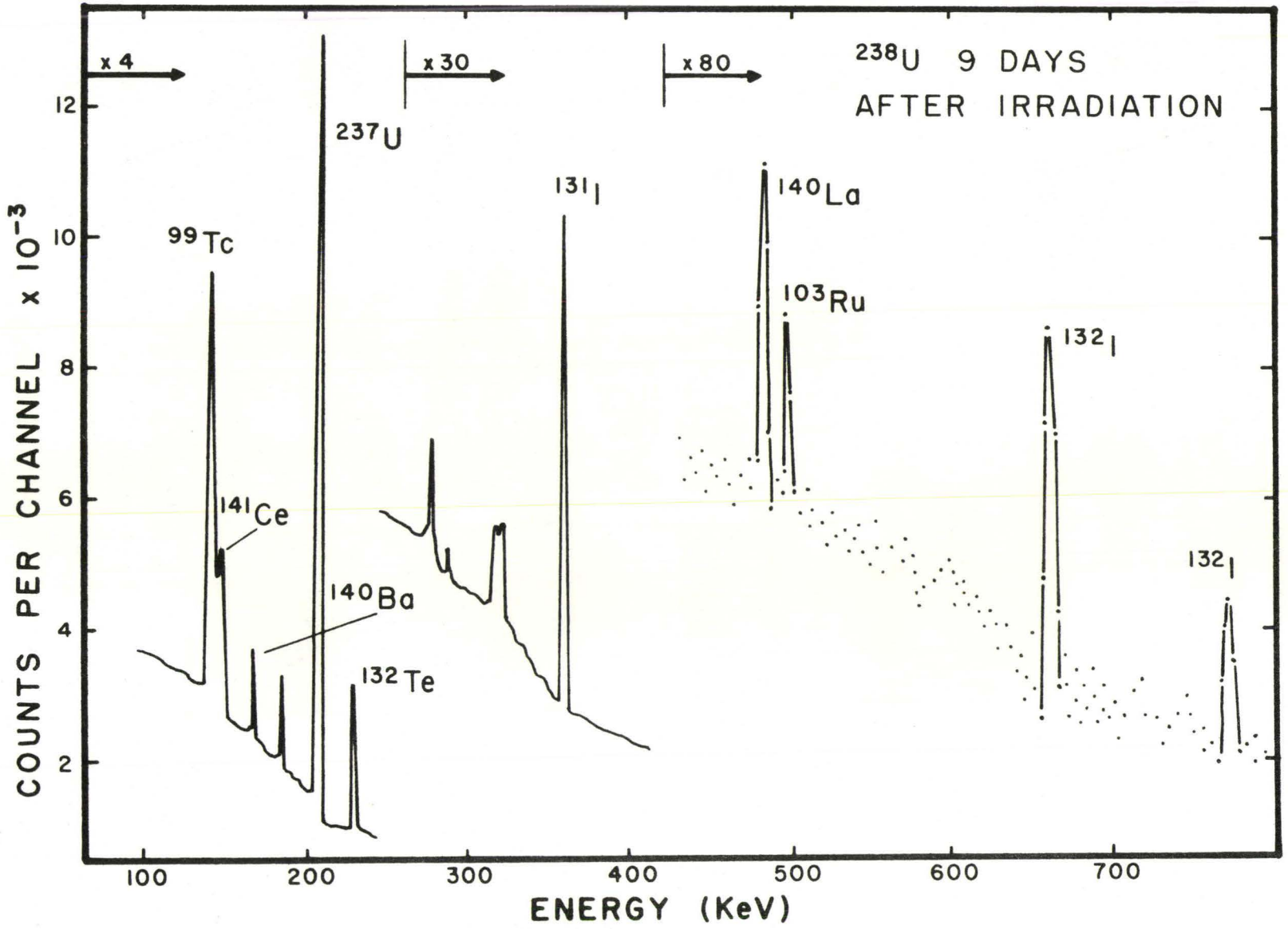
x 4
x 30
x 80
238U 9 DAYS
AFTER IRRADIATION
237U
131I
140La
99Tc
103Ru
132I
141Ce
140Ba
132I
132Te
COUNTS PER CHANNEL x 10-3
ENERGY (KeV)
2
4
6
8
10
12
100
200
300
400
500
600
700

Figure 10

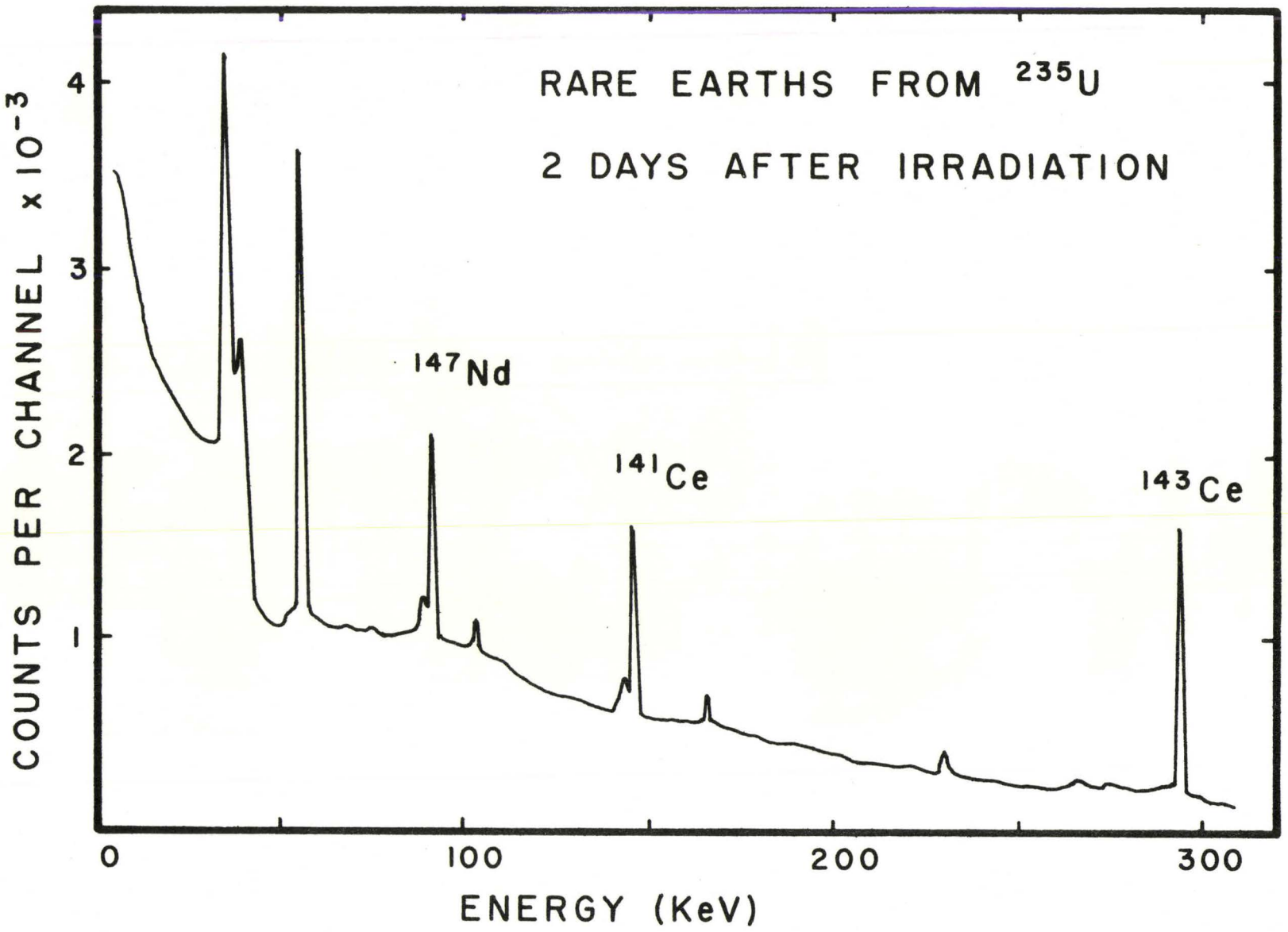
RARE EARTHS FROM ^{235}U
2 DAYS AFTER IRRADIATION
^{147}Nd
^{141}Ce
^{143}Ce
COUNTS PER CHANNEL x 10^{-3}
1
2
3
4
0
100
200
300
ENERGY (KeV)

Figure 11

measure the ^{132}Te yield. The ^{238}U spectra contain a ^{237}U peak which is produced by the (n,2n) reaction on ^{238}U. This peak does not interfere with any of the fission-product peaks.

(i) Treatment of Data

In each spectrum the peak areas were determined by summing the channels under the peak and subtracting a background which was estimated by averaging four channels on each side of the peak.

The following equation was used for determination the relative yields of nuclides with prominent gamma-ray peaks in the fission-product spectrum.

$$\frac{y_x^{238}}{y_s^{238}} = \left(\frac{y_x^{235}}{y_s^{235}}\right)\left(\frac{h_x^{238}/h_s^{238}}{h_x^{235}/h_s^{235}}\right)$$

$$= R\left(\frac{y_x^{235}}{y_s^{235}}\right) \qquad (4\text{-}10)$$

where y_x^{238} = yield of nuclide x in ^{238}U 14-Mev neutron fission

y_s^{238} = yield of standard nuclide in ^{238}U 14-Mev fission

y_x^{235} = yield of nuclide x in ^{235}U thermal fission

y_s^{235} = yield of standard nuclide in ^{235}U thermal fission

h_x^{238} = measured peak area of nuclide x in spectrum from 14-Mev fission of ^{238}U.

h_s^{238} = measured peak area of standard in ^{238}U fission

h_x^{235} = measured peak area of nuclide x in ^{235}U thermal fission spectrum

h_s^{235} = measured peak area of standard in ^{235}U fission.

The 140-keV ^{99}Tc peak was chosen as a standard in samples A, B, and C since it is prominent in the spectrum for the first two weeks

after the irradiation, during which time most of the measurements were made. Table IX gives the experimentally determined values of R along with the assumed ^{235}U fission yields and the calculated ^{238}U yields relative to ^{99}Tc.

Correction for ^{234}Th Contamination in ^{238}U

Because of the low activity of the samples it was necessary to correct for the presence of ^{234}Th contamination in samples E and F. Thorium is produced from ^{238}U by the following reaction,

$$^{238}U\ (4.507 \times 10^{9}\ yr) \xrightarrow{\alpha} {}^{234}Th\ (24.1\ d) \xrightarrow{\beta} {}^{234}Pa \rightarrow .$$

The ^{234}Th emits a gamma ray with an energy of 91 keV which is the same energy as the ^{147}Nd gamma ray. It was estimated that during the 19 hours thatelapsed between the purification of the ^{238}U and its final separation from the rare-earth fission products, enough ^{234}Th would be formed to interfere with the determination of the ^{147}Nd, as the ion-exchange procedure used would not separate thorium from the rare earths.

In order to correct for this, a sample was prepared of the same weight as samples E and F, using uranyl nitrate in which the uranium and thorium were in secular equilibrium. This sample was counted for the same length of time (4 hours), with the same geometry as the sample containing the ^{147}Nd, and the number of counts in the peak was determined.

The ^{234}Th activity at equilibrium is given by

$$\frac{dN_2}{dt} = \lambda_2 N_2 = \lambda_1 N_1 \qquad (4\text{-}11)$$

where N_1 and N_2 represent ^{238}U and ^{234}Th respectively and λ_1 and λ_2 are their respective decay constants.

TABLE IX

Results of Counting Gross Fission-Product Spectra

Mass Chain (x)	$\frac{y_x^{235}}{y_{99}^{235}}$	R	Number of Determinations	$\frac{y_x^{238}}{y_{99}^{238}}$
85 (Kr)	0.215	0.944 ± 0.033	7	0.203 ± 0.007
91 (Y)	0.964	0.691 ± 0.045	6	0.666 ± 0.043
97 (Zr; Nb)	1.005	0.954 ± 0.062	19	0.959 ± 0.062
99 (Tc)	1.000	1.000	-	1.000
103 (Ru)	0.495	1.89 ± 0.24	10	0.936 ± 0.120
131 (I)	0.484	1.46 ± 0.14	16	0.707 ± 0.068
132 (I)	0.723	1.10 ± 0.12	32	0.795 ± 0.087
133 (I)	1.092	1.01 ± 0.08	13	1.10 ± 0.09
135 (Xe)	1.064	1.04 ± 0.06	9	1.11 ± 0.06
139 (Ba)	1.059	0.861 ± 0.041	4	0.912 ± 0.043
140 (Ba,La)	1.031	0.800 ± 0.087	10	0.825 ± 0.090
143 (Ce)	0.942	0.822 ± 0.076	14	0.744 ± 0.072

Fission yields for the heavy fragments in ^{235}U fission were taken from the work of Farrar and Tomlinson[1] and those for the light fragments from Katcoff[22].

A short time after separation of the thorium from the uranium, the thorium activity in the uranium sample is given by

$$\frac{dN_2}{dt} = \lambda_1 N_1 \left[e^{-\lambda_1 t} - e^{-\lambda_2 t} \right] \qquad (4\text{-}12)$$

where t is the time elapsed since the separation.

Therefore, the ratio of the thorium activity soon after separation to the activity at equilibrium is

$$r = e^{-\lambda_1 t} - e^{-\lambda_2 t} \qquad (4\text{-}13)$$

In sample F, the time between the two separations was 19 hours; hence, r has the value 0.0225. A measurement of the activity of the ^{234}Th at equilibrium gave a value of 48246 counts per hour and thus the ^{147}Nd peak had to be reduced by 48246 x 0.0225 = 1086 counts per hour. These corrections are shown for sample F in Table X where it can be seen that they amounted to from 29 to 43 per cent of the measured peak. In the case of sample E, the correction was too large (> 90%) to be made with any accuracy and therefore, only the ^{141}Ce/^{143}Ce ratio was determined from sample E.

In samples D, E and F, the ^{99}Tc could not be used as a standard as it remained with the uranium fraction. In these samples, ^{143}Ce was taken as a secondary standard since its yield relative to ^{99}Tc was determined from samples A, B, and C. Table XI gives the relevant data from samples D, E and F.

Normalization to Mass-Spectrometric Data

The counting data was originally normalized to ^{99}Tc and the mass spectrometric data to ^{134}Xe. In the four chains which were measured by both methods, the ratio ^{99}Tc/^{134}Xe was calculated using the relation

TABLE X

Corrections to ^{147}Nd for ^{234}Th Contamination

	Counts in peak (4-hour count)				
Time from end of irradiation (hours)	36	47	64	84	93
Measured ^{147}Nd	14034	13175	11307	10940	10000
Correction for ^{234}Th	4342	4342	4342	4342	4342
Corrected ^{147}Nd	10692	8833	6965	6598	5658
% Correction	29%	33%	38%	40%	43%

TABLE XI

Results of Counting Separated Rare-Earth Fraction

Mass Chain (x)	$\frac{y_x^{235}}{y_{143}^{235}}$	R	Number of Determinations	$\frac{y_x^{238}}{y_{143}^{238}}$
141 (Ce)	1.004	1.14 ± 0.04	11	1.14 ± 0.04
143 (Ce)	1.000	1.000	-	1.00
147 (Nd)	0.378	1.26 ± 0.07	5	0.476 ± 0.026

Fission yields for ^{235}U were taken from Farrar and Tomlinson[1]

$$\left(\frac{y_x^{238}}{y_{99}^{238}}\right)_{\text{counting}} \cdot \frac{y_{99}^{238}}{y_{134}^{238}} = \left[\frac{y_x^{238}}{y_{134}^{238}}\right]_{\text{mass spec.}}$$

From the four values of $y_{99}^{238}/y_{134}^{238}$ which were obtained, a weighted average was calculated and this was used to normalize the counting data to the mass-spectrometric data. The results of the normalization calculation are shown in Table XII.

The relative yields of all nuclides that were measured are given in Tables XIII and XIV along with their standard deviations.

The relatively poor precision of the counting results is due to the inability to produce sufficiently active samples with the low neutron flux available, and to the poor counting efficiency of the Ge(Li) detector, particularly at energies above 300 kev. Counts lasting up to six hours gave only a few hundred counts in some of the higher energy peaks. The errors given for the counting results are not based on statistics, but on reproducibility in anywhere from five to thirty determinations on a peak during the course of its decay. It was possible in the case of the ^{235}U standard to produce much more active samples and this minimized the contribution of the standard to the statistical errors of the ^{238}U yields.

Absolute Yields

In order to obtain absolute yields, the relative yields of the heavy-mass fission products were normalized such that they add to 100%. In the mass region 131 - 147 only five relative yields were not experimentally determined, those of masses 138, 142, 144, 145, and 146. These were instead obtained by interpolation. Using the relative abundances of ^{153}Sm and ^{156}Eu determined by Cuninghame[25] and those of ^{121}Sn, ^{125}Sn,

TABLE XII

Normalization of ^{99}Tc to ^{134}I

X	$\left(\frac{y_X^{238}}{y_{99}^{238}}\right)$ counting	$\left(\frac{y_X^{238}}{y_{134}^{238}}\right)$ mass spec.	$\frac{y_{99}^{238}}{y_{134}^{238}}$
131	0.707 ± .068	0.618 ± .002	0.874 ± .084
132	0.795 ± .087	0.760 ± .004	0.956 ± .104
133	1.101 ± .088	0.935 ± .001	0.849 ± .067
135	1.108 ± .060	.906 ± .016	0.818 ± .044
Average			0.846 ± .032

^{127}Sb and ^{144}Ce of Ames et al.[24], all with respect to ^{140}Ba, it was possible to extrapolate the mass-yield curve to either side and obtain relative yields of masses 118 - 130 and 148 - 157. The absolute yields of the light fragments were computed using the calculated absolute yield of mass 134. The absolute yields thus obtained are given in Tables XIII and XIV and the heavy mass yields are plotted in Figure 12.

TABLE XIII

Relative and Absolute Yields of
The Light Mass Fragments in 14-Mev Fission of ^{238}U

Mass	Relative Yield	Absolute Yield (%)
83	0.115 ± 0.006	0.748 ± 0.043
84	0.194 ± 0.010	1.26 ± 0.071
85	0.172 ± 0.009	1.12 ± 0.06
86	0.271 ± 0.014	1.76 ± 0.10
91	0.563 ± 0.042	3.66 ± 0.29
97	0.811 ± 0.060	5.27 ± 0.41
99	0.846 ± 0.032	5.50 ± 0.24
103	0.792 ± 0.105	5.15 ± 0.69

TABLE XIV

Relative and Absolute Yields of
the Heavy Fragments in 14-Mev Fission of ^{238}U

Mass		Relative Yield	Absolute Yield (%)	
119 - 130	a	2.456	15.98	
131		0.618 ± 0.002	4.02 ± 0.09	
132		0.760 ± 0.004	4.94 ± 0.11	
133		0.935 ± 0.001	6.08 ± 0.14	
134		1.000	6.50 ± 0.15	
135		0.906 ± 0.016	5.89 ± 0.17	
136		0.883 ± 0.003	5.74 ± 0.13	
137		0.782 ± 0.079	5.08 ± 0.52	
138	a	0.775	5.04 ± 0.51	b
139		0.772 ± 0.047	5.02 ± 0.33	
140		0.698 ± 0.081	4.54 ± 0.53	
141		0.745 ± 0.058	4.84 ± 0.39	
142	a	0.700	4.55 ± 0.47	b
143		0.655 ± 0.066	4.26 ± 0.44	
144	a	0.549	3.57 ± 0.37	b
145	a	0.460	2.99 ± 0.31	b
146	a	0.370	2.40 ± 0.24	b
147		0.312 ± 0.036	2.03 ± 0.24	
148 - 157	a	1.010	6.53	
TOTAL		15.386	100.00	

a obtained by interpolation and extrapolation

b estimated errors

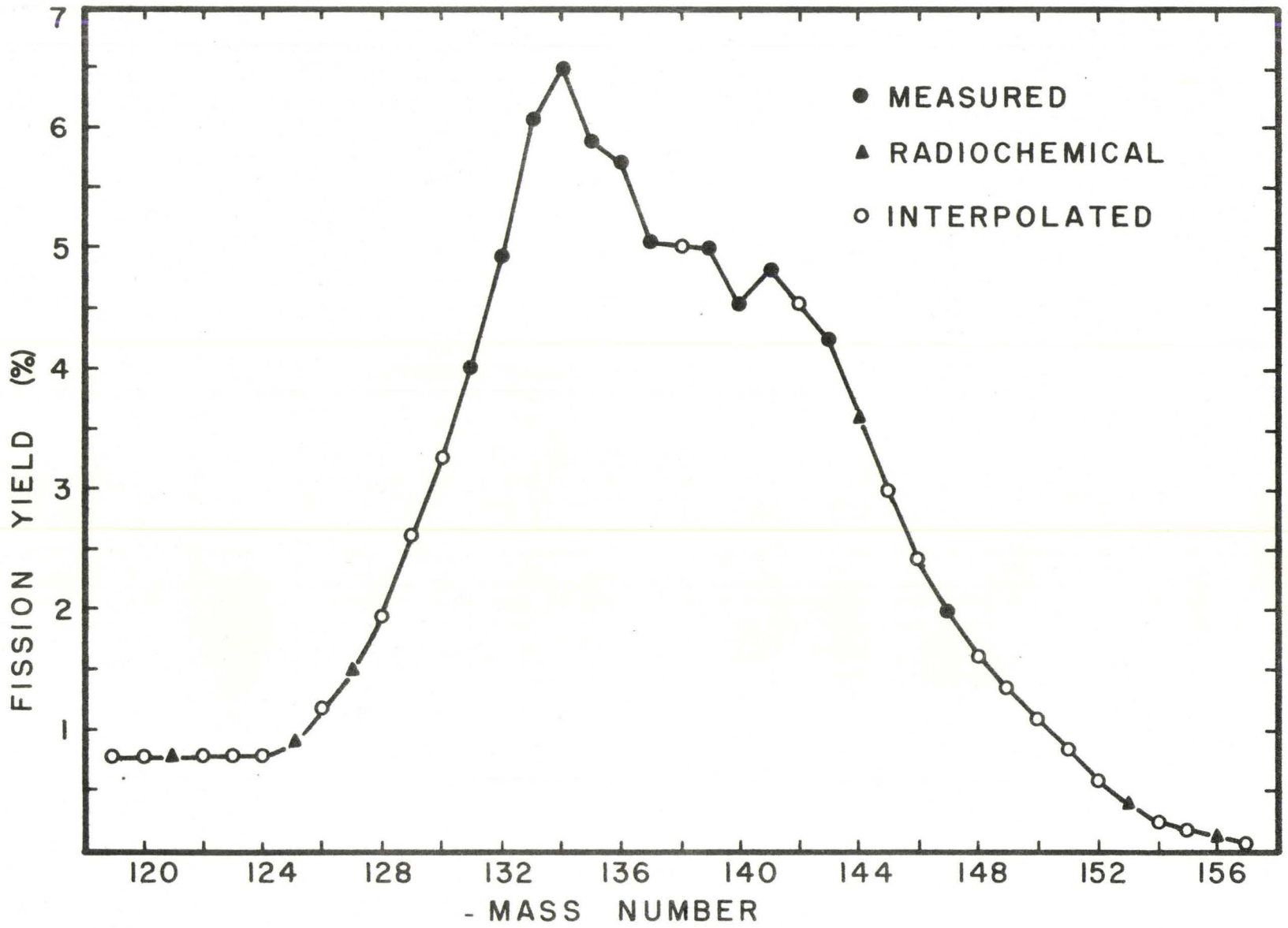

Heavy-mass yields in the 14-Mev neutron fission of ^{238}U

Figure 12

CHAPTER 5

DISCUSSION

Accuracy of the Relative Yields

The relative abundances reported in this work have been obtained by both mass-spectrometric and counting methods, both of which have their own different sources of errors.

Errors in the mass-spectrometric yields can arise through statistical and systematic errors in the measurements, and from the corrections for decay and contamination. In general, the statistical errors have been less than 1% as can be seen from the standard deviations quoted for the individual measurements. Systematic errors can arise through mass discrimination in the source and at the electron multiplier in the mass spectrometer. Clarke[50], using the same machine, has found no isotopic fractionation among the xenon isotopes and less than 1% between mass 82 and 86 among the krypton isotopes. Previous investigations[33, 51, 52] in this laboratory have shown no mass discrimination effect among the cesium isotopes. It was thus concluded that the mass discrimination effect was negligible in all cases reported here.

The correction for natural contamination involved in the xenon ratios was small, and the results from the six samples were all consistent within the quoted statistical errors. Only the ^{133}Xe and ^{135}Xe required corrections for decay and so these yields are affected by the values used for the half-lives and branching ratios. The largest uncertainty is the

correction for the independent yield of ^{135}Xe and this is responsible for the larger error given for ^{135}Xe. Including the effects of uncertainty in half-lives, branching ratios and independent yields, the ^{133}Xe and ^{135}Xe yields are believed to be reliable to 2% whereas the other xenon yields are believed to be within 1% of the true value.

Owing to the uncertain nature of the contamination correction applied to the krypton ratios, as discussed in Chapter 4, they are to be considered less accurate than the xenon ratios. Comparing the two corrections which were considered, it is unlikely that the ^{83}Kr and ^{85}Kr are in error by more than 5% while the ^{84}Kr could be in error by as much as 10%.

The statistical uncertainty (10%) in the cesium ratios is so large that effects such as mass discrimination, small errors in contamination corrections, and uncertainty in half-lives will be negligible in comparison.

There are three principal ways in which errors can arise in the yields measured by the counting technique: interference by another gamma ray of the same energy (within 1 - 2 keV), errors in the reported yields of the ^{235}U standard, and, where a chemical separation was performed, fractionation of different elements.

Interference by another gamma ray in the case of the ^{235}U is unlikely, since Gordon et al. (21) have made an extensive study of this by determining the energies and half-lives of all the peaks that were measured here, and our resolution was about the same as that reported by these authors. It is possible that in ^{238}U 14-Mev fission some nuclide (probably in the valley region) which is formed in higher yield than in ^{235}U might have a gamma ray which would interfere with one of those being measured. However, this should manifest itself in the ratio R (as defined in equation 4-10)

changing systematically with time, since it is unlikely that the interfering nuclide would have both the same gamma-ray energy and half-life as that of the one being measured. Since R remained constant within statistical errors, the measured gamma rays seemed free of interference.

The heavy-mass yields in ^{235}U thermal fission were taken from the work of Farrar and Tomlinson[1] and the errors in these are discussed elsewhere[51]. In the light mass peak the yields were normalized to the yields of Katcoff[22]. In this work these yields were considered to be exact. This is reasonable since their precision is certainly much better than the precision obtained in counting the low-activity samples obtained in this work.

The ^{147}Nd yield could be in error if, during the removal of the uranium, the neodymium and cerium somehow became partially fractionated. This is unlikely, as the anion exchange procedure used has been extensively studied[36] and the rare earths, with the exception of Ce(IV), are not adsorbed from 9M HCl solution. The presence of Ce(IV) is ruled out, as it is unstable in hydrochloric acid solution, being reduced to Ce(III) with the simultaneous liberation of chlorine[57].

In general, the relative yields from mass 131 - 136 are believed accurate to 1%, while the remaining yields in the heavy peak are thought to have an accuracy of 5 - 10%.

Contamination by ^{235}U Fission

Since natural uranium was used in the irradiations, there is the possibility that a thermal-neutron component in the 14-Mev neutron flux might cause fission in the ^{235}U that is present. This can be ruled out as a possible source of error because no ^{239}Np was observed in the 14-Mev fission-product spectrum from the ^{238}U. In a thermal neutron flux, ^{238}U

captures a neutron (σ = 2.76b)[48] to form ^{239}U which has a half-life of 23.5 m. decaying to ^{239}Np. The ^{239}Np in turn decays with a half-life of 2.33 d. to ^{239}Pu[53]. It was calculated that if no ^{239}Np were detected the thermal flux would have to be less than 10^6 n cm^{-2} sec^{-1}. Since ^{235}U comprises only 0.72% of the uranium in the sample, the maximum possible contribution from ^{235}U fission products is less than 0.5%.

Accuracy of Absolute Yields

In order to determine absolute yields, the relative yields in the heavy mass peak were normalized such that they add to 100%. This procedure necessitated interpolation of the yields at masses 138, 142, 144, 145 and 146, and extrapolation of the curve above mass 147 and below mass 131. To aid in this, radiochemical yields at masses 153, 156[25], 121, 125, 127, and 144[24] were taken relative to ^{140}Ba.

Unless there is significant fine structure at masses, 138, 142, 144, 145 and 146, it is unlikely that the interpolated yields will be systematically either high or low in comparison with the measured relative yields, and hence they will not contribute significantly to the normalization error.

The total of the measured and interpolated yields relative to ^{134}Xe given in Table XIV is 15.386; the total of the extrapolated yields is 3.466. It may, therefore, be seen that if the extrapolations had both been either high or low by 10%, the resulting error in the normalization would be only 2.3%. Although the extrapolations may be either high or low by 10%, it is unlikely that both would be high or low. Nevertheless, the 2.3% normalization error has been used.

The values of the fission yields from Table XIV are reproduced in

Table XV along with the values of Ames et al.[24], Cuninghame[25], Broom[26] and James et al[29] for comparison. In assessing these results, we must consider the fact that the relative xenon yields reported here are far superior in precision to any which have been previously reported. Therefore, the reliability of any existing data which does not have approximately the same relative yields for masses 131 - 136 must be seriously questioned.

Particular attention is drawn to the work of Broom[26, 27] whose iodine yields are in complete disagreement with this work. This author claimed to have observed a fine structure peak at A = 132; however, we find no evidence for this. On the basis of our results, the peak is definitely at mass 134, as predicted by Cuninghame[25].

The only other workers who have measured more than one yield in the region 131 - 136 are James et al.,[29] and their relative yields at 131, 133, and 135 are in general agreement with our more accurate ones. The absolute yields quoted by James et al. are believed to be somewhat less reliable than those reported here in that, although they used the same method of normalization, their measured yields amounted to only 56% out of 200%, while our measured yields totalled 59% out of 100%.

The agreement between our absolute yields and those of Cuninghame[25] is quite remarkable considering that his absolute yields were obtained by normalizing the area under the entire mass-yield curve on the basis of only twelve measured yields totalling 29% out of 200%.

It is difficult to compare the work of Ames et al.[24] to this work since very few yields are common to both, however in the cases where the same yield has been measured, the agreement seems reasonable.

In this work more consecutive heavy-mass yields have been determined

TABLE XV

Absolute Yields of Fragments in ^{238}U 14-Mev Fission

	Absolute Total Chain Yields				
Mass Chain	Ames et al. (1958)	Cuninghame (1957)	Broom (1962)	James et al. (1964)	This work
83				0.68	0.75
84				1.33	1.26
85					1.12
86					1.76
89	3.0	2.30	2.0		
90			3.4		
91		2.78	2.6		3.66
93				4.11	
97	4.8			5.97	5.27
99	5.7	5.58		6.47	5.50
103					5.15
105	3.4			2.65	
109				1.20	
111	0.87	0.81	0.6	0.98	
112				0.79	
113			0.6	0.87	
115	0.71	0.64		0.64	
121	0.73				
125	0.83				
127	1.43				
129				1.18	
131			2.7	4.60	4.02
132	4.7		4.5		4.94
133			2.6	6.65	6.08
134			4.7		6.50
135			5.0	5.59	5.89
136					5.74
137					5.08

continued . . .

TABLE XV

Absolute Yields of Fragments in ^{238}U 14-Mev Fission

Mass Chain	Ames et al. (1958)	Cuninghame (1957)	Broom (1962)	James et al. (1964)	This work
138					
139			4.4	4.92	5.02
140	4.6	4.41	4.3	4.67	4.54
141					4.84
142					
143		3.91		3.51	4.26
144	3.4	2.68			
145					
146					
147		1.99			2.03
148					
149					
150					
151					
152					
153		0.39			
154					
155					
156	0.22	0.13			
157					

than in any previous work, and, because of the methods used, the errors are more easily assessed. Although other individual radiochemical yields might prove more accurate, the data reported here should certainly give the best overall picture of the general shape of the heavy-fragment mass-yield curve.

The Nature of the Fissioning Species

Fission induced by 14-Mev neutrons is a more complicated process than thermal fission because several different reactions are possible at the higher energy. When ^{238}U captures a 14.6-Mev neutron, the resultant ^{239}U compound nucleus has an excitation energy of 19.36 Mev[58]. The ^{239}U may either fission, or emit a neutron to form ^{238}U which, in turn, may fission or emit a neutron. The possible reactions are shown in Figure 13.

Using the methods described by Hanna and Clarke[59], it is possible to calculate the cross sections for the three fission reactions and the average number of neutrons emitted in each case. The results of such a calculation are given in Table XVI.

From these results, we see that the measured mass distribution is actually a composite of the distributions from ^{239}U at 19 Mev excitation, ^{238}U at 13 Mev excitation, and ^{237}U at 6 Mev excitation. The average mass of the fissioning species is 238.3 and $\bar{\nu}$ is 3.62.

Delayed-Neutron Emission

In order to understand what happens when a nucleus undergoes fission, one should look at the prompt mass-yield curve, rather than the cumulative-yield curve, which includes the post-fission effects of prompt- and delayed-neutron emission.

The first step in constructing the prompt-yield curve is to correct

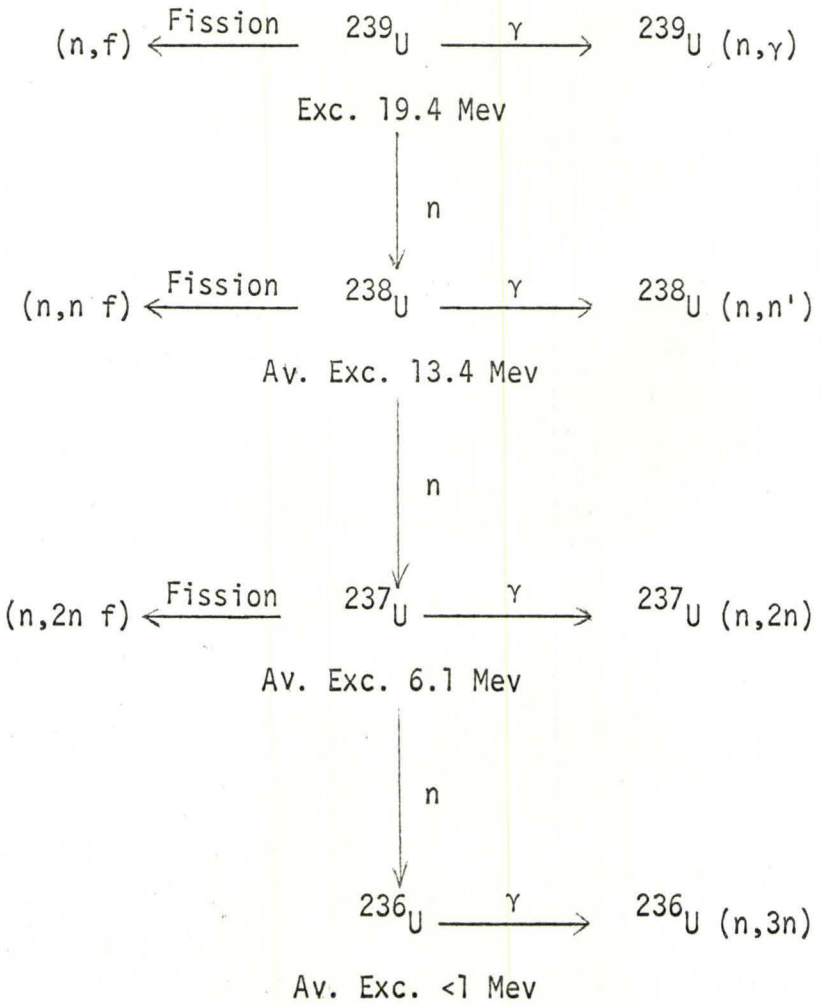

Figure 13

Reactions produced by the interaction of 14-Mev Neutrons with ^{238}U.
From Hanna and Clarke (59).

TABLE XVI

Partial cross sections and number of fission neutrons in the interaction of 14-MeV neutrons with ^{238}U

X	Nucleus	Excitation (MeV)(a)	σ(n,xn f) (barns)(b)	Number of neutrons emitted (c) following fission
0	U-239	19.36	0.55	4.30
1	U-238	13.4	0.45	3.45
2	U-237	6.1	0.25	2.41
3	U-236	$\sim$ 0	0	0

(a) Nuclear masses taken from Foreman and Seaborg[58].

(b) Cross sections from Hemmendinger[56].

(c) Assuming an average kinetic energy of 1.2 Mev for the emitted neutron [60].

the cumulative-yield curve for the effects of delayed-neutron emission. It is quite difficult to correct accurately for this, because so little information is available on the yields and neutron emission probabilities of the delayed neutron emitters in 14-Mev fission. Some yields of delayed neutron precursors have been measured by Russian workers[61,62] in 14-Mev fission of ^{238}U, but these yields are extremely high, and are not supported by the work of Hermann et al[63]. Their data is given in Table XVII.

The individual yields of delayed neutrons for ^{238}U 14-Mev fission will be different from the values in Table XX for ^{235}U thermal fission. However, the ^{235}U yields may be used to estimate the ^{238}U yields by assuming that the ^{238}U yields are greater (or smaller) in proportion to the change in cumulative yield of the chain up to and including the delayed neutron precursor. The cumulative yields may be estimated by using the hypothesis of equal charge displacement[40].

Table XVIII gives the computed absolute yield of the delayed neutron precursors for ^{235}U; and Table XIX those for ^{238}U, assuming that the fissioning nucleus has a mass of 239 and $\bar{\nu}=4.3$[59]. The calculated delayed neutron yield for ^{238}U is given in Table XX and the corrected yields for masses 136 - 139 are shown in Table XXI.

The mass yield curve, corrected for delayed-neutron emission is shown in Figure 14 along with the curves for thermal fission of ^{235}U and fast fission of ^{238}U for comparison.

Two features of the curve are particularly prominent. Firstly, the yields below mass 130 are significantly higher than in the case of ^{235}U thermal and ^{238}U fast fission; and secondly, the prominent peak at mass 134 which has been observed in fission of ^{233}U, ^{235}U, ^{238}U, ^{239}Pu and ^{241}Pu is

TABLE XVII

Absolute Abundance of Delayed Neutron Groups
^{238}U 14-Mev Fission

Group	Half Life	Measured Absolute Abundance (n/100 fissions)
1	55 s	$0.050 \pm .004$
2	22 s	$0.37 \pm .04$
3	6 s	$0.42 \pm .07$
4	2 s	~ 0.6

Table taken from Reference (63).

TABLE XVIII

Yields of Delayed Neutron Precursors in ^{235}U Fission

Delayed Neutron Precursor	Fractional Chain Yield up to and Including Precursor (a)	Absolute Total Chain Yield (%) (b)	Cumulative Yield of Precursor (%)
^{88}Br	0.78	3.49	2.7
^{137}I	0.74	6.30	4.7
^{89}Br	0.60	4.77	2.9
^{138}I	0.55	6.70	3.7
^{90}Br	0.36	5.92	2.1
^{139}I	0.31	6.51	2.0

(a) Calculated from the ECD hypothesis[40].

(b) Taken from Reference (18).

TABLE XIX

Yields of Delayed Neutron Precursors in ^{238}U 14-Mev Fission

Delayed Neutron Precursor	Fractional Chain Yield up to and Including Precursor (a)	Absolute Total Chain Yield. (%)	Cumulative Yield of Precursor. (%)
^{88}Br	0.85	2.5 (b)	2.1
^{137}I	0.79	5.08(c)	4.0
^{89}Br	0.69	3.0 (b)	2.1
^{138}I	0.60	5.04(c)	3.0
^{90}Br	0.46	3.4 (b)	1.6
^{139}I	0.37	5.02(c)	1.9

(a) Calculated using ECD hypothesis[40].

(b) Estimated on the basis of a smooth curve between measured ^{85}Kr and ^{91}Y yields.

(c) Taken from Table XIV, this work.

TABLE XX

Yields of Delayed Neutrons in ^{235}U Thermal and ^{238}U 14-Mev Fission

Group	Half-Life	Precursor	Yield in ^{235}U Fission (neutrons/100 fissions)	Yield in ^{238}U 14-Mev Fission
1	54.5 s	^{87}Br	0.058	
2	24.4 s	^{137}I	0.22	0.19
	16.3 s	^{88}Br	0.157	0.12
3	6.3 s	^{138}I	0.103	0.08
	4.4 s	$(89)_{Br}$	0.298	0.21
	6 s	$(93,94)_{Rb}$	0.001	
4	2.0 s	^{139}I	0.084	0.08
	(1.6-2.4 s)	(Cs,Sb or Te)	0.206	
	1.6 s	$(90)_{Br}$	0.236	0.18
	1.5 s	$(93)_{Kr}$	0.007	
5	0.5 s	$(^{140}I, ^{95}Kr, ^{92}Br)$	-	
	0.2 s	$(^{93}Br, ^{87,86}As, ^{97,96}Rb)$	-	

Table taken from Refence (64).

TABLE XXI

Corrections for Delayed Neutron Emission in ^{238}U 14-Mev Fission

Mass	Correction to Measured Yield	Measured Yield (%)	Corrected Yield (%)
136	- 0.19	5.74	5.55
137	+ 0.11	5.08	5.19
138	0	5.04	5.04
139	+ 0.08	5.02	5.10

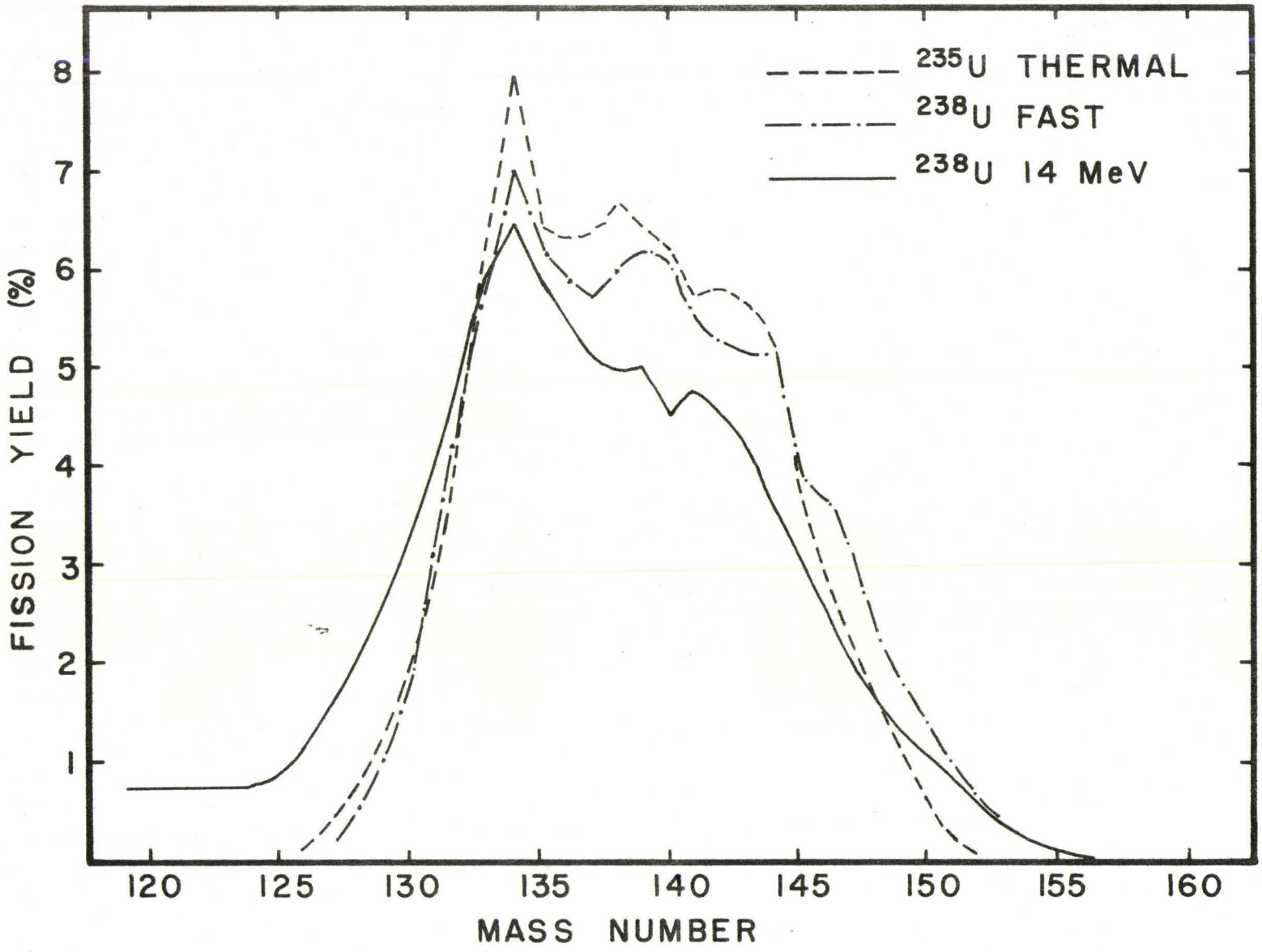

Heavy-mass yields for ^{235}U thermal, ^{238}U fast, and ^{238}U 14-Mev fission

Figure 14

still present. Although the precision of the data is not good enough to definitely establish the presence of the two smaller peaks at mass 138 and 141, it can be seen that, if they are present at all, they are much smaller than in the other two cases shown.

In order to proceed further and construct the primary-yield curve, it is necessary to know the prompt-neutron yield as a function of the mass of the fragment. Unfortunately, this has not been measured for the 14-Mev neutron fission of ^{238}U. We shall, therefore, assume a neutron distribution and, using the methods described by Terrell[65], attempt to deduce the form of the primary-yield curve.

Variation of Neutron Yield with Fragment Mass

Strong variation of neutron yield with fragment mass was first reported by Fraser and Milton[66] in 1954 for fission of ^{233}U. This was again observed by Whetstone in ^{252}Cf spontaneous fission[67] and by Apalin et al.[68] for ^{235}U thermal-neutron fission. Fickel[69], Farrar and Tomlinson[18] and Terrell[65] showed that from a knowledge of the cumulative and primary yields it was possible to deduce the neutron yield. It was shown that small changes in the slope of the neutron emission curve were sufficient to produce significant fine structure in the cumulative yield curve where none existed in the primary curve.

Terrell[65] derived neutron-yield curves for ^{233}U, ^{235}U, ^{239}Pu and ^{252}Cf. He observed that they were quite similar and could be approximated by a straight line, which in the heavy mass region has the form

$$\nu_H = 0.10\ (M_H - 126) \qquad (5\text{-}1)$$

where ν_H is the average number of neutrons emitted by a fragment of mass M_H.

Of course, this "universal" neutron emission curve will not lead to any fine structure in the cumulative yields that is not present in the primary yields, as it has a constant slope, and changes in slope are required to produce fine structure. In all of the measured curves, there is a change in slope near mass 136 and it is likely that this is connected with the magic number N = 82. In the following discussion we shall speculate as to exactly how the N = 82 shell might cause this change in slope, and we shall generate this change in slope by applying correction terms to Terrell's "universal" neutron emission curve.

As a result of the closed shell (N = 50, 82), nuclei with 51 or 83 neutrons have abnormally low binding energies (by 2 or 3 Mev) for the last neutron. It was postulated by Glendenin[15] that "a primary fission product (which has already emitted the usual number of prompt neutrons) containing one neutron in excess of the closed shell will often emit this more loosely bound neutron immediately rather than emit a beta particle or a gamma ray as in the ordinary case". This was later extended by Pappas[16] to include 3 and 5 neutrons in excess of a closed shell, as the last neutron in these cases also has an abnormally low binding energy.

These proposals have been criticized on the grounds that they would increase the yield of a specific nuclide at the expense of those higher in mass. By this mechanism a peak at A = 134 must be accompanied by a region of low yield at masses 135 - 137. This is not the case, as these yields are essentially the same as their complementary fragments[18].

However, when the Glendenin-Pappas mechanism was originally proposed there was no knowledge of the prompt neutron distribution, and it was assumed that the neutron emission probability was the same for all masses. We now

know that this is not the case, but the neutron distribution has a "saw tooth" shape, increasing approximately linearly with mass in both the light- and heavy-fragment regions[65].

In the light of this, the Glendenin-Pappas mechanism need not lead to a region of low yield above the peak, because, due to the general increase in neutron emission with mass, those nuclides in the region A = 135 - 139 could gain as much from higher masses as they lose to lower masses.

This mechanism thus can be used to explain the change in slope of the neutron emission curve in the region around A = 136.

It is, therefore, suggested that the "universal" neutron emission curve be modified by the addition of terms to take into account this added neutron emission. We write the modified equation as

$$\nu_H(M_H) = 0.10\ (M_H - 126) + \delta f_{83}(M_H) + \varepsilon f_{85}(M_H) + \gamma f_{87}(M_H) \qquad (5\text{-}2)$$

where $f_{83}(M_H)$ is the fraction of the mass chain M_H which has 83 neutrons after the "normal" prompt neutron emission has occurred; $f_{85}(M_H)$ is the fraction of the chain with 85 neutrons, and $f_{87}(M_H)$ is the fraction with 87 neutrons. δ, ε and γ are constants giving the fraction of those fragments with 83, 85 and 87 neutrons which actually emit a neutron.

As a test of equation (5-2), we shall construct the neutron emission curve for thermal neutron fission of ^{235}U. The values of f_{83} and f_{85} are given in Table XXII, along with the "normal" number of prompt neutrons emitted by each fragment (ν_p). The "normal" prompt neutron emission is calculated from the straight line $\nu_p = 0.10\ (M_H - 126)$.

The fractional chain yields f_{83} and f_{85} were calculated using Wahl's

TABLE XXII

Values of f_{83} and f_{85} for ^{235}U Thermal Fission

Mass	ν_p	f_{83}	f_{85}
130	0.4	1.1×10^{-7}	
131	0.5	3.0×10^{-6}	
132	0.6	4.0×10^{-5}	
133	0.7	0.005	
134	0.8	0.083	
135	0.9	0.151	
136	1.0	0.369	
137	1.1	0.424	0.0012
138	1.2	0.442	0.067
139	1.3	0.273	0.207
140	1.4	0.176	0.337
141	1.5	0.102	0.398
142	1.6	0.020	0.472
143	1.7	0.0012	0.424
144	1.8	-	0.244
145	1.9	-	0.176
146	2.0	-	0.067
147	2.1	-	0.005

$\nu_p = 0.10\ (M_H - 126)$

empirical Z_p values[42] and charge distribution curve[43]. The values of δ, ε, and γ were estimated by fitting the calculated curve to that of Farrar and Tomlinson[18]. The best values of the constants thus obtained are $\delta = 0.7$, $\varepsilon = 0.3$, $\gamma \simeq 0$.

Figure 15 gives the calculated neutron distribution along with the one deduced by Farrar and Tomlinson[18] from mass-yield data.

It can be seen that the deviation of the measured distribution from the straight line in the region A = 130 - 146 is reproduced remarkably well.

In theory it should be possible to calculate values for the constants, δ, ε, and γ. This requires assumptions regarding the residual energy distribution in the fragment after evaporation of the "normal" amount of neutrons, and a knowledge of neutron separation energies.

The masses and Q-values for the neutron-rich nuclides formed in fission have not been determined experimentally and must be calculated using semi-empirical mass formulae. Such calculations are not reliable in the shell regions. A comparison between experimental and calculated neutron separation energies for the few 83 neutrons nuclides for which information is available shows that the calculated values can be in error by as much as 1 Mev. Such calculations, therefore, could not be expected to provide reliable values of δ, ε, and γ.

To test the applicability of this method to other nuclei, the neutron emission curve was derived for ^{233}U, as it has approximately the same $\bar{\nu}$ as ^{235}U. From the cumulative yields of Bidinosti, Irish, and Tomlinson[70], a prompt yield curve was constructed using the methods described by Terrell[65].

These curves are shown in Figure 16 along with the prompt-yield curve given by Terrell[65]. It can be seen that the calculated prompt-yield

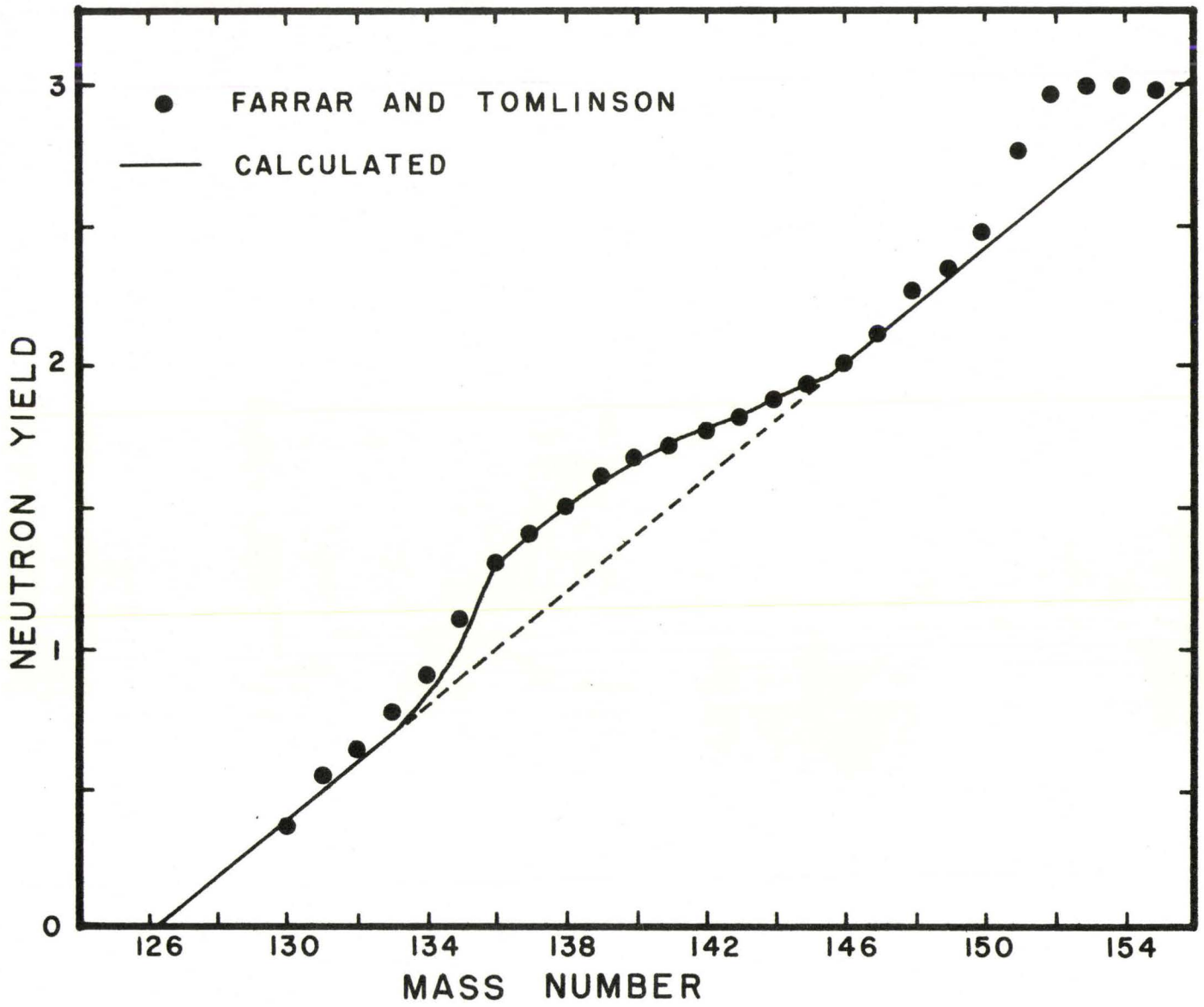

Calculated and observed neutron distribution from ^{235}U thermal fission

Figure 15

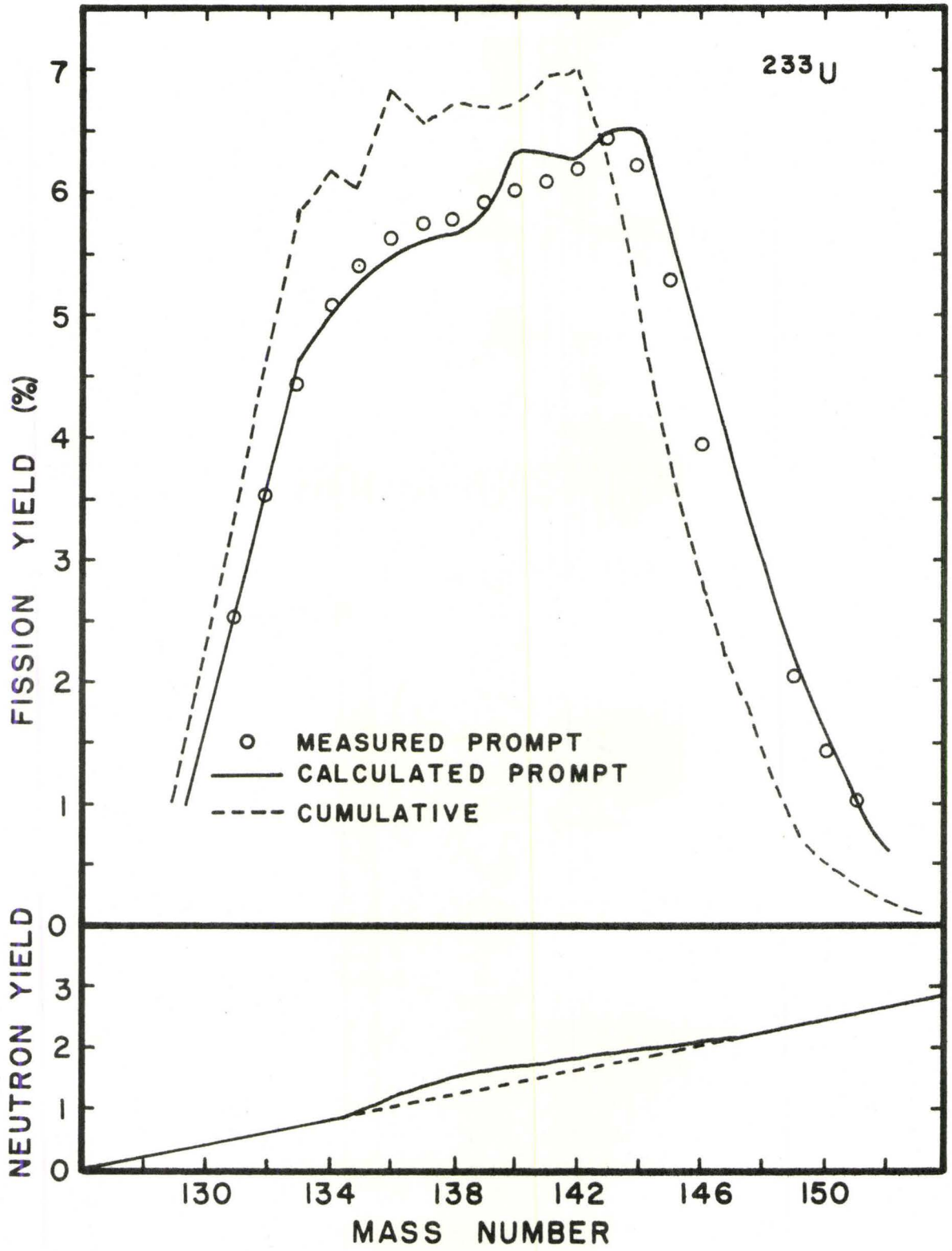

Measured and calculated prompt yields for the heavy fragments in ^{233}U fission

Figure 16

curve fits the measured one remarkably well below mass 139. Gordon et al.[21] have measured ^{233}U fission yields using a Ge(Li) detector and their results are not in agreement with the mass-spectrometric results above A = 139. They suggest that perhaps the normalization of the heavy-heavy fragments to the light-heavy fragments in the mass-spectrometric yields is in error. In the light of the good fit between the experimental and calculated prompt-yield distributions below mass 139 it is likely that they* are correct. When their results are used in the region above mass 139, the cumulative-yield curve is lowered and the calculated prompt-yield curve is in much better agreement with the experimental curve.

It therefore seems that this method is capable of predicting the prompt-yield curves for thermal-neutron fission, and we shall assume that it also applies to fission at higher excitation energies.

There are several problems to be overcome in constructing the neutron emission curve for 14-Mev neutron fission. Direct application of the "universal" curve is a dubious procedure since the "saw-tooth" shape may not persist at the higher energy, and the total neutron emission is much greater

Some information is available on the neutron distribution at higher excitation energies as a result of studies of the alpha-particle induced fission of ^{232}Th. The 27.5-Mev ^{4}He-induced fission of ^{232}Th and the 14-Mev neutron-induced fission of ^{235}U both occur from the same compound nucleus at about the same excitation energy, and thus their neutron distributions should be similar[71].

Britt and Whetstone have obtained the primary mass distribution in the 27.5-Mev ^{4}He-induced fission of ^{232}Th by measuring both the kinetic energies[71] and velocities[72] of coincident fission-fragment pairs. Neutron distributions were obtained by comparing the mass distribution from the

* Gordon et al

double-energy measurements with that from the double-velocity measurements; and, by comparing the mass distribution from the double-velocity measurements with yields obtained by radiochemical methods.

The neutron distributions obtained from these two different methods are not in agreement. The distribution obtained from comparison with radiochemical data shows the "saw tooth" behaviour exhibited in low energy fission along with a central hump in the region of symmetric fission. This is illustrated in Figure 17(a). The distribution obtained by comparison with double-energy measurements is shown in Figure 17(b). This distribution does not show the "saw tooth" behaviour.

Britt and Whetstone[71] have discussed these two neutron distributions in connection with "fragment-shell" theories and the two-mode of fission hypothesis. They conclude that the curve obtained from radiochemical and time-of-flight data is consistent with the fragment shell theories, while the two-mode hypothesis could lead to the distribution obtained from the energy measurements.

It is obvious that both of these distributions cannot be correct; however, the authors are unable to definitely choose between them.

It would appear that curve (a) is more consistent with Terrell's ideas of a "universal" neutron emission curve than curve (b). The universal curve was derived from low-energy fission data, and, because of the low symmetric fission yields, no information is available about it between masses 110 - 126. Curve (a) exhibits the saw-tooth shape, with the addition of an observable dependence in the region of symmetric fission. It is conceivable that, if the neutron distribution at low energies were examined in this region, it might exhibit the same type of dependence as curve (a).

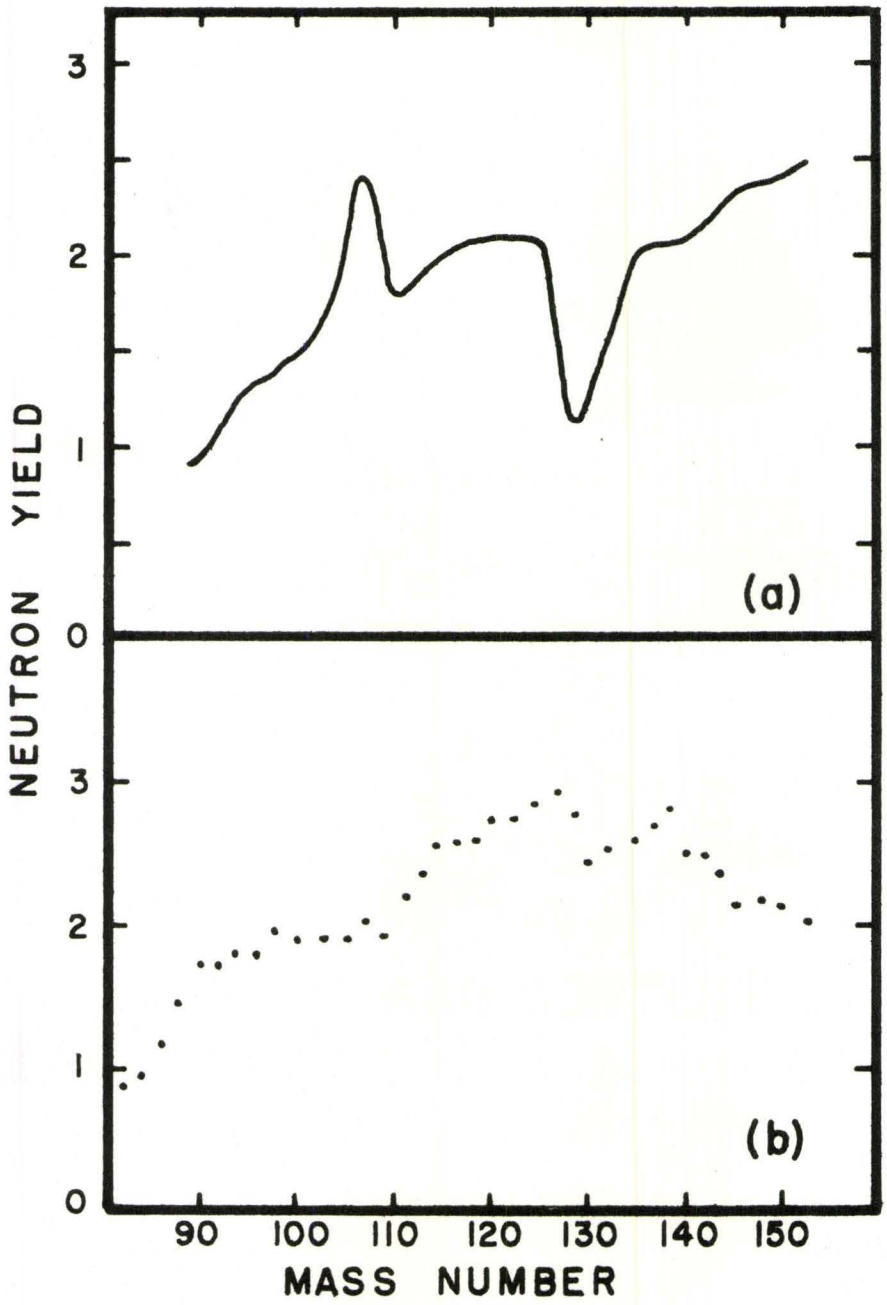

(a) Distribution obtained from comparison of radiochemical and double-velocity data[72]

(b) Distribution obtained from comparison of double-energy and double velocity data[71].

Neutron distirubtion from fission of thorium by 25.7 Mev alpha particles

Figure 17

As asymmetric fission is still predominant at 14-Mev, it is not unreasonable to assume that the neutron distribution would still exhibit the saw-tooth shape characteristic of asymmetric fission.

If there were a second, symmetric mode of fission with a neutron distribution radically different than the asymmetric mode, it is possible that the two distributions might combine to produce a curve having the form of (b). However, they might also combine to give a curve of the form of (a).

Curve (a) is thus consistent with the two-mode of fission hypothesis, yet it does not require this hypothesis to produce it.

Because curve (a) is consistent with the ideas presented in this thesis, it will be assumed that the neutron distribution from ^{238}U 14-Mev fission has the form of curve (a).

Therefore, to a first approximation, the neutron emission in the region A > 130 will be given by a straight line similar to Terrell's universal curve. The slope of this line will be increased to take into account the greater neutron emission in 14-Mev fission.

In order to determine the slope, the total number of neutrons emitted by mass 150 and its complementary light fragment was determined. This was accomplished by folding the cumulative-yield curve such that the light masses fell on top of their complementary heavy masses. It was thus determined that mass 150 and its complement emit a total of 4.5 neutrons. If we assign one of these to the light mass fragment, then mass 150 must emit an average of 3.5 neutrons. Assuming that the neutron emission goes to zero at mass 126 as in low energy fission, the slope of the line is, therefore, determined.

On the basis of these assumptions, the straight line approximation will be given by

$$\nu_H = 0.146\ (M_H - 126) \qquad (5\text{-}3)$$

Assuming that the same methods used to construct the neutron distributions for ^{235}U and ^{233}U are valid at the higher excitation energy, the neutron distribution for the heavy fragments in ^{238}U 14-Mev fission will be given by

$$\nu_H = 0.146\ (M_H - 126) +)0.7f_{83} + 0.3\ f_{85} \qquad (5\text{-}4)$$

Z_p values for ^{238}U were calculated by the displacement method[41] assuming an average fissioning mass of 239 and $\bar{\nu} = 4.32$[59]. The Z_p values used and the calculated values of f_{83} and f_{85} are given in Table XXIII. The neutron emission curve thus obtained is shown in Figure 18 along with the measured cumulative- and predicted prompt-yield curves.

The average number of neutrons emitted from the heavy fragment can be obtained from the relation,

$$\bar{\nu}_H = \frac{\sum_m \nu_m\ y_m}{\sum_m y_m} \qquad (5\text{-}5)$$

where ν_m is the average number of neutrons emitted by a heavy fragment of mass m, and y_m is the prompt yield of that fragment. This calculation gives a value of $\bar{\nu}_H = 2.1$ which is reasonable in view of the value for $\bar{\nu}(=\bar{\nu}_H + \bar{\nu}_L)$ of 4.32 given by Hanna and Clarke[59].

It is interesting that the prompt-yield curve shows three maxima, as these have been observed in the prompt-yields for thermal-neutron fission of ^{235}U and ^{233}U. The peak at A = 134 in the cumulative yields is seen to be largely due to post-fission neutron evaporation as was shown to be the case for ^{235}U[18]; however, there still appears to be a significant probability of the direct formation of fragments with mass 134 and 135.

In addition, the analysis has generated a central peak in the primary-yield curve which is not present in the cumulative yields. The washing out of this peak is likely due to the increased neutron emission at the higher excitation energy. Because of the assumptions made in this analysis, we cannot definitely state that the prompt-yield curve we have derived is the correct one. It is, therefore, highly desirable that attempts be made to measure the prompt yields directly, in order to determine whether fine structure does exist in the primary distribution as predicted by this analysis.

TABLE XXIII

Values of f_{83} and f_{85} for 14-Mev Neutron Fission of ^{238}U

Mass	*Z_p	+ν_p	f_{83}	f_{85}
132	51.0	0.88	4.0×10^{-5}	-
133	51.2	1.00	0.005	-
134	51.5	1.15	0.067	-
135	52.1	1.30	0.123	-
136	52.3	1.45	0.307	-
137	53.0	1.60	0.369	3.0×10^{-4}
138	53.2	1.75	0.472	0.020
139	53.6	1.88	0.398	0.102
140	54.1	2.04	0.273	0.207
141	54.7	2.18	0.210	0.276
142	55.1	2.33	0.083	0.424
143	55.7	2.48	0.051	0.461
144	56.1	2.62	0.003	0.442
145	56.6	2.77	-	0.369
146	57.0	2.90	-	0.210
147	57.5	3.05	-	0.035

* Reference values $Z_p(^{235}U)$ were taken from Wahl[42]

\+ $\nu_p = 0.146\ (M_H - 126)$

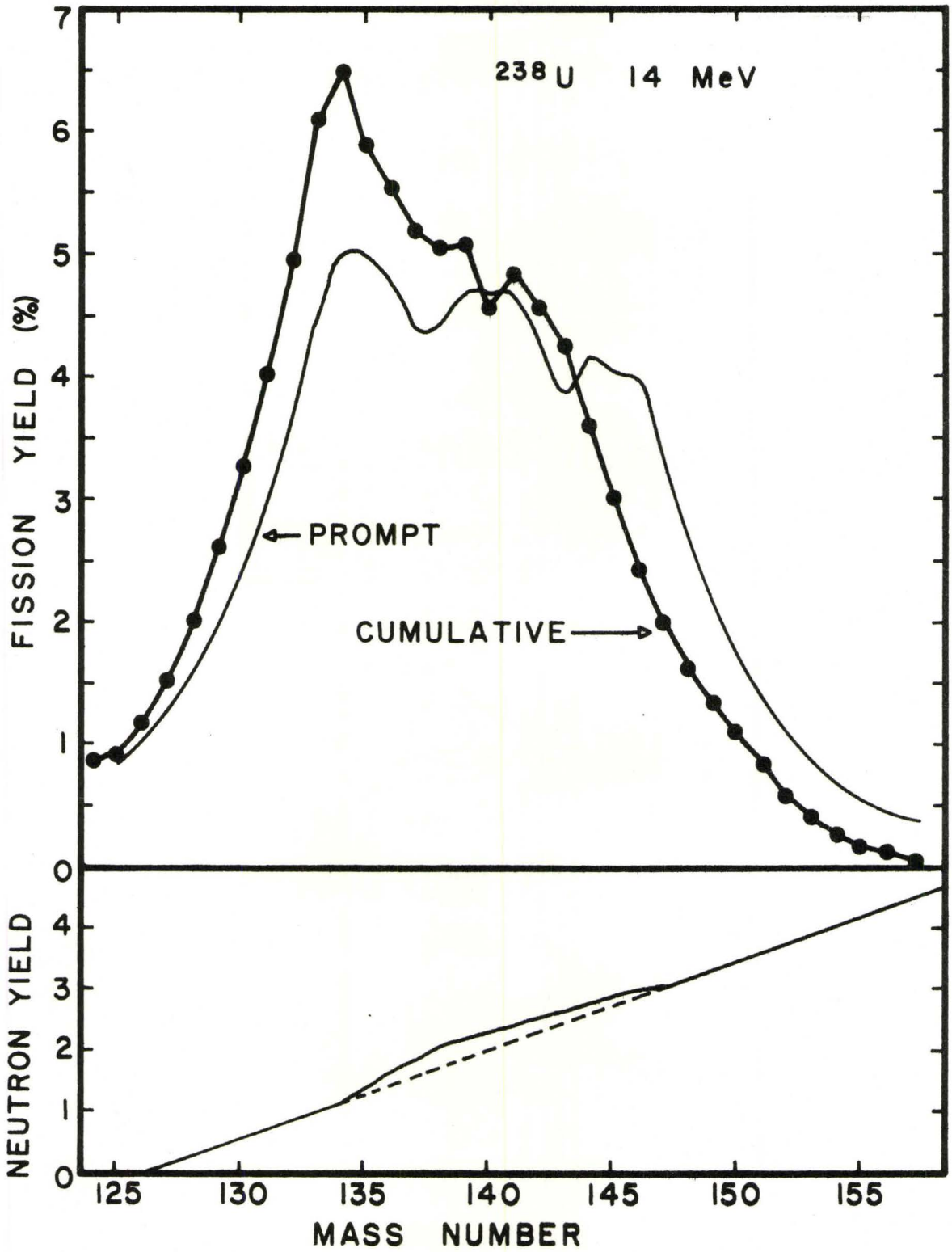

Measured cumulative- and predicted prompt-yield curve for 14-Mev neutron fission of ^{238}U.

Figure 18

APPENDIX A

Calculation of Mean Values and Standard Deviations

In each mass spectrometric sample analyzed approximately ten spectra were taken. In each spectrum the peak ratios were computed and the mean and variance calculated from the relationships

$$\bar{x}_i = \frac{1}{N} \sum_{j}^{N} x_j \qquad \text{(A-1)}$$

$$\sigma_i^2 = \frac{1}{N-1} \sum_{j}^{N} (x_j - \bar{x})^2 \qquad \text{(A-2)}$$

The final value of a particular isotopic ratio was usually determined from two or more separate samples. These were used to calculate the mean value and standard deviation from the relationships

$$\bar{R} = \frac{\sum_{i}^{m} \bar{x}_i w_i}{\sum_{i}^{m} w_i} \qquad \text{(A-3)}$$

where $w_i = \frac{1}{\sigma_i^2}$

$$\frac{1}{\sigma_{\bar{R}}^2} = \sum_{i}^{m} \frac{1}{\sigma_i^2} = \sum_{i}^{m} w_i \qquad \text{(A-4)}$$

The values quoted in the average column in the experimental results are $\bar{R}$ and $\sigma_{\bar{R}}$. The values quoted for each sample are $\bar{x}_i$ and σ_i.

In the counting experiments, the average value of R and its variance were calculated using equations (A-1) and (A-2).

APPENDIX B

Derivation of Equations for Decay of Xenon

The decay schemes for ^{135}I and ^{133}I are similar and have the form given below

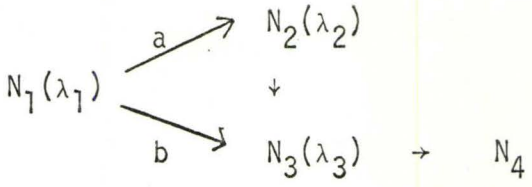

At any time during the irradiation, the differential equations of growth and decay are as follows.

$$\frac{dN_1}{dt} = R_1 - N_1\lambda_1 \qquad \text{(B-1)}$$

$$\frac{dN_2}{dt} = R_2 + aN_1\lambda_1 - N_2\lambda_2 \qquad \text{(B-2)}$$

$$\frac{dN_3}{dt} = R_3 + bN_1\lambda_1 + N_2\lambda_2 - N_3\lambda_3 \qquad \text{(B-3)}$$

Here, R_1 is the rate of formation of N_1, and R_2 and R_3 are the independent rates of formation of N_2 and N_3; a and b are the fractions of N_1 that decay to N_2 and N_3 respectively.

Equations (B-1), (B-2) and (B-3) have the following solutions for $0 \leq t \leq T$ where T is the length of the irradiation.

$$N_1 = \frac{R_1}{\lambda_1}\left[1 - e^{-\lambda_1 t}\right] \qquad \text{(B-4)}$$

$$N_2 = \frac{R_2}{\lambda_2}\left[1 - e^{-\lambda_2 t}\right] + aR_1\left[\frac{1}{\lambda_2}\left(1 - e^{-\lambda_2 t}\right) - \frac{1}{\lambda_2-\lambda_1}\left(e^{-\lambda_1 t} - e^{-\lambda_2 t}\right)\right] \quad \text{(B-5)}$$

$$N_3 = \frac{R_3}{\lambda_3}\left[1 - e^{-\lambda_3 t}\right] + (R_2 + aR_1)\left[\frac{1}{\lambda_3}\left(1 - e^{-\lambda_3 t}\right) - \frac{1}{\lambda_3-\lambda_2}\left(e^{-\lambda_2 t} - e^{-\lambda_3 t}\right)\right]$$

$$+ bR_1\left[\frac{1}{\lambda_3}\left(1 - e^{-\lambda_3 t}\right) - \frac{1}{\lambda_3-\lambda_1}\left(e^{-\lambda_1 t} - e^{-\lambda_3 t}\right)\right]$$

$$- aR_1\frac{\lambda_2}{\lambda_2-\lambda_1}\left[\frac{1}{\lambda_3-\lambda_1}\left(e^{-\lambda_1 t} - e^{-\lambda_3 t}\right) - \frac{1}{\lambda_3-\lambda_2}\left(e^{-\lambda_2 t} - e^{-\lambda_3 t}\right)\right] \quad \text{(B-6)}$$

For times (t) after the end of the irradiation and before the iodine precursor has been separated from the Xenon, R_1, R_2 and R_3 in equations (B-1), (B-2) and (B-3) vanish and the solutions are then

$$N_1 = \frac{R_1}{\lambda_1}\left[1 - e^{-\lambda_1 T}\right] e^{-\lambda_1 t} \quad \text{(B-7)}$$

$$N_2 = aR_1\left[\frac{\left(1 - e^{-\lambda_1 T}\right)}{\lambda_2 - \lambda_1} e^{-\lambda_1 t} - \frac{\lambda_1\left(1 - e^{-\lambda_2 T}\right)}{\lambda_2\left(\lambda_2 - \lambda_1\right)} e^{-\lambda_2 t}\right] + \frac{R_2}{\lambda_2}\left[1 - e^{-\lambda_2 T}\right] e^{-\lambda_2 t} \quad \text{(B-8)}$$

$$N_3 = aR_1 \left[\frac{\lambda_2 \left(1 - e^{-\lambda_1 T}\right)}{(\lambda_2-\lambda_1)(\lambda_3-\lambda_1)} e^{-\lambda_1 t} - \frac{\lambda_1 \left(1 - e^{-\lambda_2 T}\right)}{(\lambda_2-\lambda_1)(\lambda_3-\lambda_2)} e^{-\lambda_2 t} \right.$$

$$\left. + \left(\frac{1}{\lambda_3} + \frac{\lambda_1}{(\lambda_2-\lambda_1)(\lambda_3-\lambda_2)} - \frac{\lambda_2}{(\lambda_2-\lambda_1)(\lambda_3-\lambda_1)} \right)\left(1 - e^{-\lambda_3 T}\right) e^{-\lambda_3 t} \right]$$

$$+ bR_1 \left[\frac{\left(1 - e^{-\lambda_1 T}\right)}{\lambda_3 - \lambda_1} e^{-\lambda_1 t} - \frac{\lambda_1 \left(1 - e^{-\lambda_3 T}\right)}{\lambda_3 (\lambda_3 - \lambda_1)} e^{-\lambda_3 t} \right]$$

$$+ R_2 \left[\frac{\left(1 - e^{-\lambda_2 T}\right)}{\lambda_3 - \lambda_2} e^{-\lambda_2 t} - \frac{\lambda_2 \left(1 - e^{-\lambda_3 T}\right)}{\lambda_3 (\lambda_3 - \lambda_2)} e^{-\lambda_3 t} \right]$$

$$+ \frac{R_3}{\lambda_3} \left[1 - e^{-\lambda_3 T} \right] e^{-\lambda_3 t} \quad . \qquad \text{(B-9)}$$

After separation of the xenon from the iodine, the decay equations now are

$$\frac{dN_2}{dt} = - N_2 \lambda_2 \qquad \text{(B-10)}$$

$$\frac{dN_3}{dt} = N_2 \lambda_2 - N_3 \lambda_3 \qquad \text{(B-11)}$$

These have the solutions

$$N_2 = N_2^* \, e^{-\lambda_2 t_2} \qquad \text{(B-12)}$$

$$N_3 = N_3^* \, e^{-\lambda_3 t_2} + N_2^* \frac{\lambda_2}{\lambda_3 - \lambda_2} \left[e^{-\lambda_2 t_2} - e^{-\lambda_3 t_2} \right] \qquad \text{(B-13)}$$

where t_2 is the time from separation of the xenon from the iodine, and N^*_2

and N^*_3 are the values of N_2 and N_3 at the time of separation (given by making the substitution $t \rightarrow t_1$ in equations (B-8) and (B-9)).

APPENDIX C

Calculation of the Independent Yield of Xe^{135}

A. Equal Charge Displacement (ECD) (40)

According to this hypothesis, the most probable charges of a given fission fragment and its complementary fragment lie an equal number of beta-decays from stability.

$$Z_A - Z_p = Z_A^* - Z_p^* \qquad \text{(C-1)}$$

where Z_A and Z_A^* are the most stable charges and Z_p and Z_p^* are the most probable charges for mass A and A^* respectively.

$$Z_p + Z_p^* = Z_f \qquad \text{(C-2)}$$

$$A + A^* = A_f - \nu \qquad \text{(C-3)}$$

where Z_f and A_f are the charge and mass of the fissioning nucleus and ν is the number of neutrons emitted per fission.

The most probable charge of a fission product of mass A is then given by

$$Z_p = Z_A - \frac{1}{2}(Z_A + Z_A^* - Z_f) \qquad \text{(C-4)}$$

Values of the most stable charge Z_A were taken from the compilation of Glendenin, Coryell and Edwards (40); ν for 14-Mev fission of ^{238}U was taken as 4.5 (44, 45, 46).

The result of this calculation is shown as method 1 in Table C-I.

B. Coryell Displacement Method (41)

This method is based upon the ECD hypothesis and relates $Z_p(A)$ data

for various types of fission differing in compound nucleus and excitation energy. The Z_p function for thermal neutron fission of ^{235}U is used as a reference curve and the shift in the Z_p function, called $\Delta Z_p(A)$ is computed for other systems from the following relations.

$$Z_p(A) = Z_p(A)^{235} + \Delta Z_p(A) \qquad \text{(C-5)}$$

$$\Delta Z_p(A) = \frac{1}{2}(Z_c - 92) - 0.21\,(A_c - 236) + 0.19\,(v_T - v_T^{235}) \qquad \text{(C-6)}$$

In ^{235}U thermal fission $v_T = 2.47 \pm .03$ (44) and for ^{238}U 14-Mev fission $v_T = 4.45 \pm .10$ (44). Using these values $-\Delta Z_p(A) = 0.25 \pm .02$.

$$Z_p(A) = Z_p(A)^{235} - 0.25$$

The value of $Z_p(A)^{235}$ was estimated in three different ways:

(1) $Z_p(A)^{235}$ was computed from the ECD method (40). The result of this calculation is shown as method 2 in Table C-I.

(2) Wahl's empirical $Z_p(A)^{235}$ was used (42) with the value 52.40 ± 0.15. This is shown as method 3 in Table C-I

(3) The value of $Z_p(A)^{235}$ was taken from Wahl's empirical curve (42) to give a value of 52.24. This is method 4 in Table C-I.

In each case, the yield value was taken from the charge distribution curve as given by Wahl (43).

Table C-I

Estimated Fractional Chain Yield of ^{135}Xe

Method	Z_A	Z_p	$Z - Z_p$	Fractional Chain Yield
1. ECD	55.8	52.0	2.0	0.020
2. Displacement + ECD		51.95	2.05	0.015
3. Displacement + empirical Z_p		52.15	1.85	0.045
4. Displacement + Z_p from curve		52.0	2.0	0.020
Average				0.030
Standard Deviation				0.015

BIBLIOGRAPHY

1. Farrar, H., and Tomlinson, R. H., Nucl. Phys. 34, 367-381 (1962).
2. Farrar, H. and Tomlinson, R. H., Can. J. Phys. 40, 1017 (1962).
3. Mathews, C. K., Ph.D. Thesis, McMaster University, October, 1964.
4. Hahn, O., and Strassmann, F., Naturwiss. 27, 11, 89 (1939).
5. Coryell, C., and Sugarman, N., Radiochemical Studies: The Fission Products. National Nuclear Energy Series, McGraw-Hill, New York (1951).
6. Steinberg, E. P., Glendenin, L. E., Inghram, M. G., and Hess, D. C., Phys. Rev. 95, 867 (1954).
7. Petruska, J. A., Thode, H. G., and Tomlinson, R. H., Can. J. Phys. 33, 693 (1955).
8. Thode, H. G. and Graham, R. L., Can. J. Res. A25, 1 (1947).
9. MacNamara, J., Collins, C. B., and Thode, H. G., Phys. Rev. 78, 129 (1950).
10. Fleming, W., Tomlinson, R. H., and Thode, H. G., Can. J. Phys. 32, 522 (1954).
11. Wanless, R. K., and Thode, H. G., Can. J. Phys. 33, 541 (1955).
12. Fleming, W. H. and Thode, H. G., Can. J. Chem. 34, 193 (1956).
13. Fickel, H. R. and Tomlinson, R. H., Can. J. Phys. 37, 926 (1959).
14. Farrar, H., Clarke, W. B., Thode, H. G., and Tomlinson, R. H., Can. J. Phys. 42, 2063 (1964).
15. Glendenin, L. E. Laboratory for Nuclear Science, M. I. T. Technical Report No. 35. (December 1949).
16. Pappas, A. C., Laboratory for Nuclear Science, M. I. T. Technical Report No. 63. (September 1953).
17. Wiles, D. R., Smith, B. W., Horsley, R., and Thode, H. G., Can. J. Phys. 31, 419 (1953).
18. Farrar, H., and Tomlinson, R. H., Can. J. Phys. 40, 943 (1962).
19. Ewan, G. T. and Tavendale, A. J. Can. J. Phys. 2286 (1964).

20. Banham, M. F., Fudge, A. J., and Howes, J. H., Analyst 91, 180 (1966).

21. Gordon, G. E., Harvey, J. W., and Nakahara, H., Nucleonics 24 (12), 62 (1966).

22. Katcoff, S., Nucleonics 18 (11), 201 (1960).

23. Wahl, A. C., Phys. Rev. 99, 730 (1955).

24. Ames, D. P., Balagna, J. P., Barnes, J. W., Comstock, A. A., Cowan, G. A., Elkin, P. B., Ford, G. P., Gilmore, J. S., Hoffman, D. C., Knobelock, G. W., Lang, E. J., Melnick, M. A., Minkkinen, C. D., Pollock, B. D., Sattizahn, J. E., Stanley, C. W. and Waren, B. LA-1997 (declassified 1958).

25. Cuninghame, J. G., J. Inorg. and Nucl. Chem. 5, 1 (1957).

26. Broom, K. M., Phys. Rev. 126, 627 (1962).

27. Broom, K. M., M.Sc. Thesis, University of Arkansas (1961). U. S. AEC Report No. ORO-435.

28. Broom, K. M., Phys. Rev. 133, B874 (1964).

29. James, R. H., Martin, G. R., Silvester, D. J., Radiochimica Acta. 3, 1/2, 76 (1964).

30. Clarke, W. B., Ph.D. Thesis, McMaster University, September(1962).

31. Reynolds, J. M., Rev. Sci. Instru. 27, 928 (1956).

32. Katz, J. J. and Rabinowitch, E., The Chemistry of Uranium, The Element, Its Binary and Related Compounds. National Nuclear Energy Series, McGraw-Hill. New York (1951).

33. Irish, D. E., M.Sc. Thesis, McMaster University, September (1956).

34. Inghram, M. and Chupka, W., Rev. Sci. Instr. 24 (7), 518 (1953).

35. Rodden, C. J. (ed.) Analytical Chemistry of the Manhattan Project NNES, Division VIII, Vol I. McGraw-Hill, 1950, p. 18.

36. Kraus, K. A. and Nelson, F., Proceedings of the International Conference on the Peaceful Uses of Atomic Energy, Geneva, 1955. Vol. 7, p. 113, paper 837.

37. Classen, H. H., Weinstock, B. and Malm, J. G., J. Chem. Phys. 25, 426 (1956).

38. Arendt, J. W., Powell, E. W., Saylor, H. W., AEC Report. K-1323 (1957).

39. Llewellyn, D. R., J. Chem. Soc. (London). Part 1, 28 (1953).

40. Glendenin, L. E., Coryell, C. D. and Edwards, R. R., paper 52 in Radiochemical Studies: The Fission Products. National Nuclear Energy Series. McGraw-Hill, New York (1951).

41. Coryell, C. D., Kaplan, M., and Fink, R. D., Can. J. Chem. 39, 646 (1961).

42. Wahl, A. C., Ferguson, R. L., Nethaway, D. R., Troutner, D. E. and Wolfsberg, K., Phys. Rev. 126, 1112 (1962).

43. Wahl, A. C., J. Inorg. Nucl. Chem. 6, 263 (1958).

44. Argonne National Laboratory, Reactor Physics Constants, U. S. AEC Report ANL - 5800.

45. Flerov, N. N. and Talyzin, V. M., Soviet J. Atomic Energy 5, 1593 (1958).

46. Flerov, N. N., and Tamanov, E. A., Soviet J. Atomic Energy 5, 1596 (1958).

47. Friedlander, G., Friedman, L., Gordon, B., and Yaffe, L., Phys. Rev., 129, 1809 (1963).

48. Sullivan, W. H., Trilinear Chart of the Nuclides (revised to 1962).

49. Ganapathy, R., and Ihochi, H., J. Inorg. and Nucl. Chem. 28, 3071 (1966).

50. Clarke, W. B. Private communication.

51. Farrar, H., Ph.D. Thesis, McMaster University, May, 1962.

52. Harvey, J. W., Ph.D. Thesis, McMaster University, May, 1965.

53. Hyde, E. K., Perlman, I., and Seaborg, G. T., The Nuclear Properties of the Heavy Elements, 3 volumes, Prentice-Hall (1964).

54. Hawkings, R. C., Edwards, W. J. and McLeod, E. M., Tables of Gamma Rays from the Decay of Radionuclides. AECL - 1225 (1961).

55. Table of Cross Sections for Fast Neutron Reactions. Texas Nuclear Corp., second edition, January (1964).

56. Hemmendinger, A., Second International Conference on the Peaceful Uses of Atomic Energy. Geneva (1958). P/663.

57. Kolthoff, I. M., and Sandell, E. B., Textbook of Quantitative Inorganic Analysis. (3rd edition). MacMillan (New York) p. 581.

58. Foreman, B. M. and Seaborg, G. T., J. Inorg. Nucl. Chem. 7, 305 (1958).

59. Hanna, G. C. and Clarke, R. L., Can. J. Phys. 39, 967 (1961).

60. Wolfsberg, K., Phys. Rev. 137, B929 (1965).

61. Maksyutenko, B. P., Z. Eksp. Teor. Fiz. 35, 815 (1958); English translation: Soviet Physics. JETP 35, 565 (1958).

62. Maksyutenko, B. P., Atomnaya Energiya 7, 474 (1959).

63. Hermann, G., Fiedler, J., Benedict, G., Eckhardt, W., Luthardt, G., Patzelt, P., and Schüssler, H. D. Procedings of the Symposium on Physics and Chemistry of Fission. Saltzburg, 1965. IAEA, (Vienna), 1965. vol. 2, p. 197.

64. Keepin, G. R., Nucleonics 20, (8), 150 (1962).

65. Terrell, J., Phys. Rev. 127, 880 (1962).

66. Fraser, J. S. and Milton, J. C. D., Phys. Rev. 93, 818 (1954).

67. Whetstone, S. L., Phys. Rev. 114, 581 (1959).

68. Apalin, V. F., Dobrynin, Yu. P., Zakharova, V. P., Kutikov, I. E., and Mikaelyan, L. A., Atomnaya Energ. 8, 15 (1960); English translation: Soviet J. Atomic Energy 8, 10 (1961).

69. Fickel, H. R., Ph.D. Thesis, McMaster University, 1959.

70. Bidinosti, D. R., Irish, D. E., and Tomlinson, R. H., Can. J. Chem. 39, 628 (1961).

71. Britt, H. C. and Whetstone, S. L., Phys. Rev. 133, B603 (1964).

72. Whetstone, S. L., Phys. Rev. 133, B613 (1964).